THE EUROPEAN
PHYSICAL JOURNAL C

Semileptonic and nonleptonic weak decays of $\psi(1S, 2S)$ and $\eta_c(1S, 2S)$ to $D_{(s)}$ in the covariant light-front approach

Zhi-Jie Sun, Zhi-Qing Zhang[a], **You-Ya Yang, Hao Yang**

School of Sciences, Institute of Theoretical Physics, Henan University of Technology, Zhengzhou 450052, Henan, China

Abstract In addition to the strong and electromagnetic decay modes, the $\psi(1S, 2S)$ and $\eta_c(1S, 2S)$ can also decay via the weak interaction. Such weak decays can be detected by the high-luminosity heavy-flavor experiments. At present, some of the semileptonic and nonleptonic J/Ψ weak decays have been measured at BESIII. Researching for these charmonium weak decays to $D_{(s)}$ meson can provide a platform to check of the standard model (SM) and probe new physics (NP). So we investigate the semileptonic and nonleptonic weak decays of $\psi(1S, 2S)$ and $\eta_c(1S, 2S)$ to $D_{(s)}$ within the covariant light-front quark model (CLFQM). With form factors of the transitions $\psi(1S, 2S) \rightarrow D_{(s)}$ and $\eta_c(1S, 2S) \rightarrow D_{(s)}$ calculated under the CLFQM, we predict and discuss some physical observables, such as the branching ratios, the longitudinal polarizations f_L and the forward–backward asymmetries A_{FB}. One can find that the Cabibbo-favored semi-leptonic decay channels $\psi(1S, 2S) \rightarrow D_s^- \ell^+ \nu_\ell$ with $\ell = e, \mu$ and the nonleptonic decay modes $\psi(1S, 2S) \rightarrow D_s^- \rho^+$ have relatively large branching ratios of the order $\mathcal{O}(10^{-9})$, which are most likely to be accessible at the future high-luminosity experiments.

1 Introduction

The $\psi(1S, 2S)$ and $\eta_c(1S, 2S)$ are S-wave charmonium states below the open-charm kinematic threshold. They predominantly decay through the strong and electromagnetic interactions. By contrast, their weak decays are rare processes due to the smallness of the weak interaction strength. While such decays have evoked a lot of interest from theoretical research [1–6], because they build a bridge between perturbative and nonperturbative physics and provide a valuable platform to comprehend the intricate behaviors and dynamics of strong interactions. The hadronic decays of these char-

monia via the annihilation of $c\bar{c}$ to gluons are of a high order in strong coupling α_s and are severely suppressed by the phenomenological Okubo–Zweig–Iizuka (OZI) rule [7–9]. Numerically the total branching ratio of the charmoium weak decays was estimated to be at the order of 10^{-8} [10]. New physics may have a chance to show up in such rare decays. Furthermore, for the weak decays of charmonia $\psi(1S, 2S)$, the polarization effect may play an important role to probe the underlying dynamics and hadron structures [10].

The BESIII Collaboration has reported on the results of searches for the hadronic and semileptonic weak decays $J/\psi \rightarrow D_s^- \pi^+$, $J/\psi \rightarrow D^- \pi^+$, $J/\psi \rightarrow \bar{D}^0 \bar{K}^0$ [11], $J/\psi \rightarrow D_s^- \rho^+$ [12], $J/\psi \rightarrow D_s^{(*)-} e^+ \nu_e$ [13], $J/\psi \rightarrow D^- e^+ \nu_e$ [14], respectively. Very recently, the semileptonic weak decay $J/\psi \rightarrow D^- \mu^+ \nu_\mu$ was firstly researched at BESIII [15]. The branching ratios at 90% confidence level were found to be $\mathcal{B}r(J/\psi \rightarrow D_s^- \pi^+) < 1.4 \times 10^{-4}$, $\mathcal{B}r(J/\psi \rightarrow D^- \pi^+) < 7.5 \times 10^{-5}$, $\mathcal{B}r(J/\psi \rightarrow \bar{D}^0 \bar{K}^0) < 1.7 \times 10^{-4}$, $\mathcal{B}r(J/\psi \rightarrow D_s^- \rho^+) < 1.3 \times 10^{-5}$, $\mathcal{B}r(J/\psi \rightarrow D_s^{(*)-} e^+ \nu_e) < 1.3 \times 10^{-6}$, $\mathcal{B}r(J/\psi \rightarrow D^- e^+ \nu_e) < 7.1 \times 10^{-8}$ and $\mathcal{B}r(J/\psi \rightarrow D^- \mu^+ \nu_\mu) < 5.6 \times 10^{-7}$. Certainly, these upper limits greatly exceed the predicted values within the Standard Model (SM), which are in the order of $10^{-9} \sim 10^{-12}$ [1,2,5,6,16–23]. Even so, with the significant annual accumulation of $10^{10} J/\psi$ events, BESIII will soon be capable of detecting some of these decays in the near future.

For the semileptonic decays, the hadronic transition matrix element between the initial and final mesons is most crucial for the theoretical calculations, which can be characterized by several form factors. As to the form factors, they can be extracted from data or relied on some non-perturbative methods. The covariant light-front quark model (CLFQM) as one of popular non-perturbative methods has been successfully used to calculate the form factors [24–29]. Compared with the semileptonic decays, the nonleptonic decays are more complex in dynamics due to both of the two final

states being hadrons, where more long distance effects are involved. The factorization assumption based on the vacuum saturation approximation is often used to simplify the calculations. Specifically, the matrix elements are factorized into a product of two single matrix elements of currents, where one is parameterized by the decay constant of the emitted meson and the other is represented by the transition form factors. In a word, the form factors are important to both semileptonic and nonleptonic decays. A variety of models have been applied to study the transition form factors, such as the Bauer–Stech–Wirbel (BSW) model [16], the QCD sum rules (QCDSR) [3,4,18], the Bethe-Salpeter (BS) method [19]. Based on the form factors and helicity formalisms, we also calculate another two physical observables: the forward–backward asymmetry A_{FB} and the longitudinal polarization fraction f_L, respectively.

This paper is organized as follows. The formalism of the CLFQM, the hadronic matrix elements and the helicity amplitudes combined via form factors are listed in Sect. 2. In addition to the numerical results for the $\psi(1S, 2S) \to D_{(s)}$ and $\eta_c(1S, 2S) \to D_{(s)}$ transition form factors, the branching ratios, the forward–backward asymmetries A_{FB} and the longitudinal polarization fractions f_L for the corresponding decays are presented in Sect. 3. Detailed comparisons with other theoretical values and relevant discussions are also included. The summary is presented in Sect. 4. Some specific rules when performing the p^- integration and the expression for each form factor are collected in the Appendix A and B, respectively.

2 Formalism

2.1 The form factors

The Bauer–Stech–Wirble (BSW) form factors for the $\eta_c \to D_{(s)}$ and $J/\psi \to D_{(s)}$ transitions are defined as follows[1],

$$
\langle D_{(s)}\left(P''\right)\left|V_\mu\right| \eta_c\left(P'\right)\rangle = \left(P_\mu - \frac{m_{\eta_c}^2 - m_{D_{(s)}}^2}{q^2}q_\mu\right)
$$
$$
\times F_1^{\eta_c D_{(s)}}\left(q^2\right) + \frac{m_{\eta_c}^2 - m_{D_{(s)}}^2}{q^2}q_\mu F_0^{\eta_c D_{(s)}}\left(q^2\right), \quad (1)
$$
$$
\langle D_{(s)}\left(P''\right)\left|V_\mu - A_\mu\right| J/\psi\left(P', \epsilon\right)\rangle
$$
$$
= -\epsilon_{\mu\nu\alpha\beta}\epsilon_{J/\psi}^\nu q^\alpha P^\beta \frac{V\left(q^2\right)}{m_{J/\psi} + m_{D_{(s)}}}
$$
$$
-i\frac{2m_{J/\psi}\epsilon_{J/\psi}\cdot q}{q^2}q_\mu A_0\left(q^2\right)
$$
$$
-i\epsilon_{J/\psi,\mu}\left(m_{J/\psi} + m_{D_{(s)}}\right) A_1\left(q^2\right)
$$

---

[1] It is similar for the $\eta_c(2S) \to D_{(s)}$ and $\psi(2S) \to D_{(s)}$ transitions.

$$
-i\frac{\epsilon_{J/\psi}\cdot q}{m_{J/\psi} + m_{D_{(s)}}}P_\mu A_2\left(q^2\right)
$$
$$
+i\frac{2m_{J/\psi}\epsilon_{J/\psi}\cdot q}{q^2}q_\mu A_3\left(q^2\right), \quad (2)
$$

where $P = P' + P'', q = P' - P''$ and the convention $\epsilon_{0123} = 1$ is adopted. In order to calculate the amplitudes of the transition form factors, we need the following Feynman rules for the meson–quark–antiquark vertex $i\Gamma'_M$, where the subscript M represents a pseudoscalar (P) or vector (V) meson

$$
i\Gamma'_P = H'_P\gamma_5, \quad (3)
$$
$$
i\Gamma'_V = iH'_V\left[\gamma_\mu - \frac{1}{W'_V}\left(p'_1 - p_2\right)_\mu\right]. \quad (4)
$$

The results of the lowest order form factors could be obtained by calculating the Feynman diagram shown in Fig. 1, where the Feynman diagram for the charmonium decay is also included. In the covariant quark model, the treatment of transition form factor is relatively covariant throughout the calculation process, where the light-front coordinates of a momentum p are used $p = (p^-, p^+, p_\perp)$ with $p^\pm = p^0 \pm p_z, p^2 = p^+p^- - p_\perp^2$.

The incoming (outgoing) meson has the mass M' (M'') with the momentum $P' = p'_1 + p_2$ ($P'' = p''_1 + p_2$), where $p_1^{'('')}$ and p_2 are the momenta of the quark and anti-quark inside the incoming (outgoing) meson with the mass $m_1^{'('')}$ and m_2, respectively. Here we use the same notations as those in Refs. [24,30] and M' refers to the charmonium mass. These momenta can be expressed in terms of the internal variables $(x_i, p'_\perp)$ as

$$
p_{1,2}^{'+} = x_{1,2}P'^+, \quad p'_{1,2\perp} = x_{1,2}P'_\perp \pm p'_\perp, \quad (5)
$$

with $x_1 + x_2 = 1$. Using these internal variables, we can define some quantities for the incoming meson which will be used in the following calculations

$$
M_0'^2 = \left(e'_1 + e_2\right)^2 = \frac{p_\perp'^2 + m_1'^2}{x_1} + \frac{p_\perp^2 + m_2^2}{x_2},
$$
$$
\widetilde{M}'_0 = \sqrt{M_0'^2 - \left(m'_1 - m_2\right)^2},
$$
$$
e_i^{(')} = \sqrt{m_i^{(')2} + p_\perp'^2 + p_z'^2},
$$
$$
p'_z = \frac{x_2 M'_0}{2} - \frac{m_2^2 + p_\perp'^2}{2x_2 M'_0}, \quad (6)
$$

where M'_0 is the kinetic invariant mass of the incoming meson and can be expressed as the energies of the quark and the anti-quark $e_i^{(')}$. It is similar to the case of the outgoing meson. For the general $\eta_c(1S, 2S) \to D_{(s)}$ transition, the corresponding the matrix element is

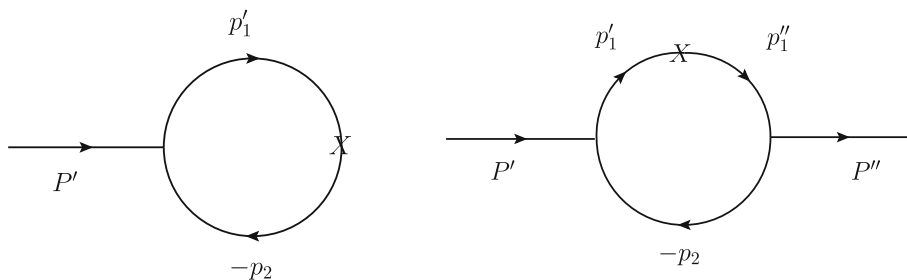**Fig. 1** Feynman diagrams for charmonium decay (left) and transition (right) amplitudes, where $P'^{('')}$ is the incoming (outgoing) meson momentum, $p_1'^{('')}$ is the quark momentum, p_2 is the anti-quark momentum and X denotes the vector or axial-vector transition vertex. One can fix the shape parameter through the left Feynman diagram

$$
\begin{aligned}
\mathcal{B}_\mu^{\eta_c D_{(s)}} &= \langle D_{(s)}\left(P''\right)|V_\mu - A_\mu|\eta_c\left(P'\right)\rangle \\
&= -i^3 \frac{N_c}{(2\pi)^4}\int d^4 p_1' \frac{H'_{\eta_c} H''_{D_{(s)}}}{N_1' N_1'' N_2} S_\mu^{\eta_c D_{(s)}},
\end{aligned} \tag{7}
$$

where $N_1'^{('')} = p_1'^{('')2} - m_1'^{('')2}$ and $N_2 = p_2^2 - m_2^2$ arise from the quark propagators, and the trace $S_\mu^{\eta_c D_{(s)}}$ can be directly obtained by using the Lorentz contraction,

$$
\begin{aligned}
S_\mu^{\eta_c D_{(s)}} &= \mathrm{Tr}\left[\gamma_5\left(\slashed{p}_1'' + m_1''\right)\gamma_\mu\left(\slashed{p}_1' + m_1'\right)\right. \\
&\quad \left.\times \gamma_5\left(-\slashed{p}_2 + m_2\right)\right].
\end{aligned} \tag{8}
$$

It is similar for the $\psi(1S, 2S) \to D_{(s)}$ transition amplitude,

$$
\mathcal{B}_\mu^{\psi D_{(s)}} = -i^3 \frac{N_c}{(2\pi)^4}\int d^4 p_1' \frac{H'_\psi\left(i H''_{D_{(s)}}\right)}{N_1' N_1'' N_2} S_{\mu\nu}^{\psi D_{(s)}} \varepsilon^{*\nu}, \tag{9}
$$

where

$$
\begin{aligned}
S_{\mu\nu}^{\psi D_{(s)}} &= \left(S_V^{\psi D_{(s)}} - S_A^{\psi D_{(s)}}\right)_{\mu\nu} \\
&= \mathrm{Tr}\left[\left(\gamma_\nu - \frac{1}{W_V''}\left(p_1'' - p_2\right)_\nu\right)\right. \\
&\quad \times \left(\slashed{p}_1'' + m_1''\right)\left(\gamma_\mu - \gamma_\mu \gamma_5\right)\left(\slashed{p}_1' + m_1'\right) \\
&\quad \left.\times \gamma_5\left(-\slashed{p}_2 + m_2\right)\right].
\end{aligned} \tag{10}
$$

The specific expressions for $S_\mu^{\eta_c D_{(s)}}$ and $S_{\mu\nu}^{\psi D_{(s)}}$ are listed in the Appendix B. In practice, we use the light-front decomposition of the Feynman loop momentum and integrate out the minus component through the contour integral method. If the covariant vertex functions are not singular when performing integration, the transition amplitudes will pick up the singularities in the anti-quark propagators. The integration then leads to

$$
\begin{aligned}
N_1'^{('')} &\to \hat{N}_1'^{('')} = x_1\left(M'^{('')2} - M_0'^{('')2}\right), \\
H_M'^{('')} &\to h_M'^{('')}, \\
W_M'' &\to w_M'', \int \frac{d^4 p_1'}{N_1' N_1'' N_2} H_P' H_M'' S^{PM}
\end{aligned}
$$

$$
\to -i\pi \int \frac{dx_2 d^2 p_\perp'}{x_2 \hat{N}_1' \hat{N}_1''} h_P' h_M'' \hat{S}^{PM}, \tag{11}
$$

where

$$
M_0''^2 = \frac{p_\perp''^2 + m_1''^2}{x_1} + \frac{p_\perp''^2 + m_2^2}{x_2}, \tag{12}
$$

with $p_\perp'' = p_\perp' - x_2 q_\perp$. The explicit forms of h_M' and w_M' are given by [24]

$$
h_P' = h_V' = \left(M'^2 - M_0'^2\right)\sqrt{\frac{x_1 x_2}{N_c}}\frac{1}{\sqrt{2}\widetilde{M}_0'}\varphi', \tag{13}
$$

$$
w_V' = M_0' + m_1' + m_2, \tag{14}
$$

with φ' being the light-front momentum distribution amplitude for the S-wave mesons,

$$
\varphi' = \varphi'\left(x_2, p_\perp'\right) = 4\left(\frac{\pi}{\beta'^2}\right)^{\frac{3}{4}}\sqrt{\frac{dp_z'}{dx_2}}\exp\left(-\frac{p_z'^2 + p_\perp'^2}{2\beta'^2}\right), \tag{15}
$$

where β' is a phenomenological parameter and can be fixed by fitting the corresponding decay constant. As to the radially excited charmonia $\psi(2S)$ and $\eta_c(2S)$, the distribution functions are given as

$$
\begin{aligned}
\varphi'(2S) &= 4\left(\frac{\pi}{\beta'^2}\right)^{\frac{3}{4}}\sqrt{\frac{dp_z'}{dx_2}}\exp\left(-\frac{p_z'^2 + p_\perp'^2}{2\beta'^2}\right) \\
&\quad \times \frac{1}{\sqrt{6}}\left(-3 + 2\frac{p_z'^2 + p_\perp'^2}{\beta'^2}\right).
\end{aligned} \tag{16}
$$

Using Eqs. (7)–(12) and taking the integration rules given in Refs. [24,30], we can obtain the $\eta_c(1S, 2S) \to D_{(s)}$ and $\psi(1S, 2S) \to D_{(s)}$ transition form factors, which are shown in the Appendix B.

2.2 Helicity amplitudes and observables

Since the form factors involving the fitted parameters for the $\eta_c(1S, 2S) \to D_{(s)}$ and $\psi(1S, 2S) \to D_{(s)}$ transitions

have been investigated in above subsection, it is convenient to obtain the differential decay widths of these semileptonic $\eta_c(1S, 2S)$ and $\psi(1S, 2S)$ decays by the combination of the helicity amplitudes via form factors, which are listed as follows

$$
\begin{aligned}
&\frac{d\Gamma(\eta_c \to D_{(s)}\ell\nu_\ell)}{dq^2} \\
&= \left(\frac{q^2 - m_\ell^2}{q^2}\right)^2 \frac{\sqrt{\lambda(m_{\eta_c}^2, m_{D_{(s)}}^2, q^2)}G_F^2|V_{CKM}|^2}{384 m_{\eta_c}^3 \pi^3} \times \frac{1}{q^2} \\
&\quad \times \left\{(m_\ell^2 + 2q^2)\lambda(m_{\eta_c}^2, m_{D_{(s)}}^2, q^2)F_1^2(q^2) \right. \\
&\quad \left. + 3m_\ell^2(m_{\eta_c}^2 - m_{D_{(s)}}^2)^2 F_0^2(q^2)\right\},
\end{aligned} \tag{17}
$$

$$
\begin{aligned}
&\frac{d\Gamma_L(\psi \to D_{(s)}\ell\nu_\ell)}{dq^2} \\
&= \left(\frac{q^2 - m_\ell^2}{q^2}\right)^2 \frac{\sqrt{\lambda(m_\psi^2, m_{D_{(s)}}^2, q^2)}G_F^2|V_{CKM}|^2}{384 m_\psi^3 \pi^3} \\
&\quad \times \frac{1}{q^2}\left\{3m_\ell^2\lambda(m_\psi^2, m_{D_{(s)}}^2, q^2)A_0^2(q^2) \right. \\
&\quad + \frac{m_\ell^2 + 2q^2}{4m_{D_{(s)}}^2}\left| (m_\psi^2 - m_{D_{(s)}}^2 - q^2)(m_\psi + m_{D_{(s)}})A_1(q^2) \right. \\
&\quad \left. \left. - \frac{\lambda(m_\psi^2, m_{D_{(s)}}^2, q^2)}{m_\psi + m_{D_{(s)}}}A_2(q^2)\right|^2\right\},
\end{aligned} \tag{18}
$$

$$
\begin{aligned}
&\frac{d\Gamma_\pm(\psi \to D_{(s)}\ell\nu_\ell)}{dq^2} \\
&= \left(\frac{q^2 - m_\ell^2}{q^2}\right)^2 \frac{\sqrt{\lambda(m_\psi^2, m_{D_{(s)}}^2, q^2)}G_F^2|V_{CKM}|^2}{384 m_\psi^3 \pi^3} \\
&\quad \times \left\{(m_\ell^2 + 2q^2)\lambda(m_\psi^2, m_{D_{(s)}}^2, q^2) \right. \\
&\quad \left. \times \left| \frac{V(q^2)}{m_\psi + m_{D_{(s)}}} \mp \frac{(m_\psi + m_{D_{(s)}})A_1(q^2)}{\sqrt{\lambda(m_\psi^2, m_{D_{(s)}}^2, q^2)}}\right|^2\right\},
\end{aligned} \tag{19}
$$

where $\lambda(q^2) = \lambda(m_{\eta_c(\psi)}^2, m_{D_{(s)}}^2, q^2) = (m_{\eta_c(\psi)}^2 + m_{D_{(s)}}^2 - q^2)^2 - 4m_{\eta_c(\psi)}^2 m_{D_{(s)}}^2$ and m_ℓ is the mass of the lepton ℓ with $\ell = e, \mu$.[2] It is noted that although the electron and nuon are very light compared with the charm quark, we do not ignore their masses in our calculations in order to check the mass effects. The combined transverse and total differential decay

widths are defined as

$$
\frac{d\Gamma_T}{dq^2} = \frac{d\Gamma_+}{dq^2} + \frac{d\Gamma_-}{dq^2}, \quad \frac{d\Gamma}{dq^2} = \frac{d\Gamma_L}{dq^2} + \frac{d\Gamma_T}{dq^2}. \tag{20}
$$

For the $\psi(1S, 2S)$ decays, it is meaningful to define the polarization fraction due to the existence of different polarizations

$$
f_L = \frac{\Gamma_L}{\Gamma_L + \Gamma_+ + \Gamma_-}. \tag{21}
$$

As to the forward–backward asymmetry, the analytical expression is defined as [31]

$$
\begin{aligned}
A_{FB} &= \frac{\int_0^1 \frac{d\Gamma}{d\cos\theta}d\cos\theta - \int_{-1}^0 \frac{d\Gamma}{d\cos\theta}d\cos\theta}{\int_{-1}^1 \frac{d\Gamma}{d\cos\theta}d\cos\theta} \\
&= \frac{\int b_\theta(q^2)dq^2}{\Gamma_{\eta_c(\psi)}},
\end{aligned} \tag{22}
$$

where θ is the angle between the 3-momenta of the lepton ℓ and the initial meson in the $\ell\nu$ rest frame. The function $b_\theta(q^2)$ represents the angular coefficient, which can be written as [31]

$$
\begin{aligned}
b_\theta(q^2) &= \frac{G_F^2|V_{CKM}|^2}{128\pi^3 m_{\eta_c}^3}q^2\sqrt{\lambda(q^2)}\left(1 - \frac{m_\ell^2}{q^2}\right)^2 \\
&\quad \times \frac{m_\ell^2}{q^2}(H_{V,0}^s H_{V,t}^s),
\end{aligned} \tag{23}
$$

$$
\begin{aligned}
b_\theta(q^2) &= \frac{G_F^2|V_{CKM}|^2}{128\pi^3 m_\psi^3}q^2\sqrt{\lambda(q^2)}\left(1 - \frac{m_\ell^2}{q^2}\right)^2 \\
&\quad \times \left[\frac{1}{2}(H_{V,+}^2 - H_{V,-}^2) + \frac{m_\ell^2}{q^2}(H_{V,0}H_{V,t})\right],
\end{aligned} \tag{24}
$$

where the helicity amplitudes

$$
\begin{aligned}
H_{V,0}^s\left(q^2\right) &= \sqrt{\frac{\lambda(q^2)}{q^2}}F_1\left(q^2\right), \\
H_{V,t}^s\left(q^2\right) &= \frac{m_{\eta_c}^2 - m_{D_{(S)}}^2}{\sqrt{q^2}}F_0\left(q^2\right),
\end{aligned} \tag{25}
$$

for the $\eta_c(1S, 2S) \to D_{(s)}$ transitions, and the helicity amplitudes

$$
\begin{aligned}
H_{V,\pm}\left(q^2\right) &= (m_\psi + m_{D_{(s)}})A_1\left(q^2\right) \mp \frac{\sqrt{\lambda(q^2)}}{m_\psi + m_{D_{(s)}}}V\left(q^2\right), \\
H_{V,0}\left(q^2\right) &= \frac{m_\psi + m_{D_{(s)}}}{2m_\psi\sqrt{q^2}}\left[-\left(m_\psi^2 - m_{D_{(s)}}^2 - q^2\right)\right. \\
&\quad \left. \times A_1\left(q^2\right) + \frac{\lambda(q^2)A_2(q^2)}{(m_\psi + m_{D_{(s)}})^2}\right], \\
H_{V,t}\left(q^2\right) &= -\sqrt{\frac{\lambda(q^2)}{q^2}}A_0\left(q^2\right),
\end{aligned} \tag{26}
$$

---

[2] From now on, we use ℓ to represent e, μ for simplicity.

for the $\psi(1S, 2S) \to D_{(s)}$ transitions. Here the subscript V in each helicity amplitude refers to the $\gamma_\mu(1 - \gamma_5)$ current.

2.3 Hadronic matrix elements

In phenomenology, the effective Hamiltonian of charmomium weak decays $\psi(1S, 2S) \to D_{(s)}M$ and $\eta_c(1S, 2S) \to D_{(s)}M$ with $M = \pi, K, \rho, K^*$ can be written as [32]

$$\mathcal{H}_{\text{eff}} = \frac{G_F}{\sqrt{2}} \sum_{q_1, q_2} V_{cq_1}^* V_{uq_2} \{C_1(\mu)Q_1(\mu) + C_2(\mu)Q_2(\mu)\} + \text{H.c.} \quad (27)$$

where G_F is the Fermi coupling constant, $V_{cq_1}^* V_{uq_2}$ is the product of the CKM matrix elements with $q_{1(2)} = s, d$, and $C_{1,2}(\mu)$ are the Wilson coefficients. The local tree four-quark operators $Q_{1,2}$ are defined by

$$Q_1 = \left[\bar{q}_{1,\alpha}\gamma_\mu (1 - \gamma_5) c_\alpha\right]\left[\bar{u}_\beta\gamma^\mu (1 - \gamma_5) q_{2,\beta}\right], \quad (28)$$
$$Q_2 = \left[\bar{q}_{1,\alpha}\gamma_\mu (1 - \gamma_5) c_\beta\right]\left[\bar{u}_\beta\gamma^\mu (1 - \gamma_5) q_{2,\alpha}\right], \quad (29)$$

where α and β are color indices. Based on the effective Hamiltonian and the naive factorization approach, the matrix elements for the decays $\eta_c(1S, 2S) \to D_{(s)}M$ can be expressed as

$$\mathcal{A}\left(\eta_c \to D_{(s)}M\right) = \langle D_{(s)}M | \mathcal{H}_{\text{eff}} | \eta_c \rangle$$
$$= \frac{G_F}{\sqrt{2}} V_{cq_1}^* V_{uq_2} a_1 \langle M | J^\mu | 0 \rangle \langle D_{(s)} | J_\mu | \eta_c \rangle, \quad (30)$$

where the combination of the Wilson coefficients $a_1 = C_1 + C_2/3$ and $\langle M | J^\mu | 0 \rangle$ is defined as $\langle P(q) | A^\mu | 0 \rangle = -if_P q_\mu$ for pseudoscalar (P) mesons and $\langle V(q, \epsilon) | V^\mu | 0 \rangle = f_V m_V \epsilon_\mu^*$ for vector (V) mesons. Specifically, the total amplitude for each decay channel can be further written as follows

$$\mathcal{A}\left(\eta_c \to D_s^- \pi^+\right)$$
$$= i \frac{G_F}{\sqrt{2}} V_{ud} V_{cs}^* a_1 \left(m_{\eta_c}^2 - m_{D_s}^2\right) f_\pi F_0^{\eta_c D_s}\left(m_\pi^2\right), \quad (31)$$
$$\mathcal{A}\left(\eta_c \to D_s^- K^+\right)$$
$$= i \frac{G_F}{\sqrt{2}} V_{us} V_{cs}^* a_1 \left(m_{\eta_c}^2 - m_{D_s}^2\right) f_K F_0^{\eta_c D_s}\left(m_K^2\right), \quad (32)$$
$$\mathcal{A}\left(\eta_c \to D^- \pi^+\right)$$
$$= i \frac{G_F}{\sqrt{2}} V_{ud} V_{cd}^* a_1 \left(m_{\eta_c}^2 - m_D^2\right) f_\pi F_0^{\eta_c D}\left(m_\pi^2\right), \quad (33)$$
$$\mathcal{A}\left(\eta_c \to D^- K^+\right)$$
$$= i \frac{G_F}{\sqrt{2}} V_{us} V_{cd}^* a_1 \left(m_{\eta_c}^2 - m_D^2\right) f_K F_0^{\eta_c D}\left(m_K^2\right), \quad (34)$$
$$\mathcal{A}\left(\eta_c \to D_s^- \rho^+\right)$$
$$= \sqrt{2}G_F V_{ud} V_{cs}^* a_1 m_\rho \left(\epsilon_\rho^* \cdot p_{\eta_c}\right) f_\rho F_1^{\eta_c D_s}\left(m_\rho^2\right), \quad (35)$$

$$\mathcal{A}\left(\eta_c \to D_s^- K^{*+}\right)$$
$$= \sqrt{2}G_F V_{us} V_{cs}^* a_1 m_{K^*} \left(\epsilon_{K^*}^* \cdot p_{\eta_c}\right) f_{K^*} F_1^{\eta_c D_s}\left(m_{K^*}^2\right), \quad (36)$$
$$\mathcal{A}\left(\eta_c \to D^- \rho^+\right)$$
$$= \sqrt{2}G_F V_{ud} V_{cd}^* a_1 m_\rho \left(\epsilon_\rho^* \cdot p_{\eta_c}\right) f_\rho F_1^{\eta_c D}\left(m_\rho^2\right), \quad (37)$$
$$\mathcal{A}\left(\eta_c \to D^- K^{*+}\right)$$
$$= \sqrt{2}G_F V_{us} V_{cd}^* a_1 m_{K^*} \left(\epsilon_{K^*}^* \cdot p_{\eta_c}\right) f_{K^*} F_1^{\eta_c D}\left(m_{K^*}^2\right). \quad (38)$$

In addition, the amplitudes for the decays $\psi(1S, 2S) \to D_{(s)}P$ with $P = \pi, K$ can be expressed as

$$\mathcal{A}(\psi \to D_{(s)}P) = \langle D_{(s)}P | \mathcal{H}_{eff} | \psi \rangle$$
$$= \frac{G_F}{\sqrt{2}} V_{cq_1}^* V_{uq_2} a_1 2m_\psi \left(\epsilon_\psi \cdot p_P\right) f_P A_0^{\psi D_{(s)}}\left(m_P^2\right). \quad (39)$$

As to the specific decay channels, the amplitudes are given as

$$\mathcal{A}\left(\psi \to D_s^- \pi^+\right)$$
$$= \sqrt{2}G_F V_{ud} V_{cs}^* a_1 m_\psi \left(\epsilon_\psi \cdot p_\pi\right) f_\pi A_0^{\psi D_s}\left(m_\pi^2\right), \quad (40)$$
$$\mathcal{A}\left(\psi \to D_s^- K^+\right)$$
$$= \sqrt{2}G_F V_{us} V_{cs}^* a_1 m_\psi \left(\epsilon_\psi \cdot p_K\right) f_K A_0^{\psi D_s}\left(m_K^2\right), \quad (41)$$
$$\mathcal{A}\left(\psi \to D^- \pi^+\right)$$
$$= \sqrt{2}G_F V_{ud} V_{cd}^* a_1 m_\psi \left(\epsilon_\psi \cdot p_\pi\right) f_\pi A_0^{\psi D}\left(m_\pi^2\right), \quad (42)$$
$$\mathcal{A}\left(\psi \to D^- K^+\right)$$
$$= \sqrt{2}G_F V_{us} V_{cd}^* a_1 m_\psi \left(\epsilon_\psi \cdot p_K\right) f_K A_0^{\psi D}\left(m_K^2\right). \quad (43)$$

For the decays $\psi(1S, 2S) \to D_{(s)}V$, the hadronic matrix elements can be expressed as

$$\mathcal{A}\left(\psi \to D_{(s)}V\right) = \langle D_{(s)}V | \mathcal{H}_{\text{eff}} | \psi \rangle$$
$$= \frac{G_F}{\sqrt{2}} V_{cq_1}^* V_{uq_2} a_1 H_\lambda, \quad (44)$$

where λ denotes the helicity of vector meson, and $H_\lambda = \langle V | J^\mu | 0 \rangle \langle D_{(s)} | J_\mu | \psi \rangle$ is given as follows

$$H_0 \equiv \langle V\left(\varepsilon_0', p_V\right) |\bar{q}\gamma^\mu q| 0 \rangle$$
$$\langle D_{(s)}\left(p_{D_{(s)}}\right) |\bar{c}\gamma_\mu (1 - \gamma_5) b| \psi\left(\varepsilon_0, p_\psi\right) \rangle$$
$$= \frac{if_V}{2m_\psi}\left[\left(m_\psi^2 - m_{D_{(s)}}^2 + m_V^2\right)\left(m_\psi + m_{D_{(s)}}\right) A_1^{\psi D_{(s)}}\left(m_V^2\right) \right.$$
$$\left. + \frac{4m_\psi^2 p_c^2}{m_\psi + m_{D_{(s)}}} A_2^{\psi D_{(s)}}\left(m_V^2\right) \right], \quad (45)$$
$$H_\pm \equiv \langle V\left(\varepsilon_\pm', p_V\right) |\bar{q}\gamma^\mu q| 0 \rangle$$
$$\langle D_{(s)}\left(p_{D_{(s)}}\right) |\bar{c}\gamma_\mu (1 - \gamma_5) b| \psi\left(\varepsilon_\pm, p_\psi\right) \rangle$$

Table 1 The values of the input parameters [29,33–37]

Mass (GeV)	$m_b = 4.8$	$m_c = 1.4$	$m_s = 0.37$	$m_{u,d} = 0.25$	$m_e = 0.000511$
	$m_\pi = 0.140$	$m_K = 0.494$	$m_\rho = 0.775$	$m_{K^*} = 0.892$	$m_\mu = 0.106$
	$m_{\eta_c} = 2.9839$	$m_{J/\psi} = 3.0969$	$m_{\eta_c(2S)} = 3.6377$	$m_{\psi(2S)} = 3.68610$	$m_D = 1.86966$
	$m_{D_s} = 1.96835$				
CKM		$V_{cd} = 0.221 \pm 0.004$		$V_{us} = 0.2243 \pm 0.0008$	
		$V_{ud} = 0.97373 \pm 0.00031$		$V_{cs} = 0.975 \pm 0.006$	
Decay constants (GeV)	$f_\pi = 0.132$	$f_K = 0.16$	$f_\rho = 0.209$	$f_{K^*} = 0.217$	
	$f_{J/\psi} = 0.431$	$f_{\eta_c} = 0.387$	$f_D = 0.235$	$f_{D_s} = 0.290$	
Shape parameters (GeV)	$\beta'_{\eta_c} = 0.754^{+0.014}_{-0.014}$	$\beta'_{\eta_c(2S)} = 0.388^{+0.092}_{-0.096}$	$\beta'_D = 0.541^{+0.043}_{-0.042}$		
	$\beta'_{J/\psi} = 0.646^{+0.041}_{-0.041}$	$\beta'_{\psi(2S)} = 0.385^{+0.049}_{-0.068}$	$\beta'_{D_s} = 0.645^{+0.136}_{-0.117}$		
Full width		$\Gamma_{\eta_c} = (32.0 \pm 0.7)\text{MeV}$		$\Gamma_{J/\psi} = (92.6 \pm 1.7)\text{keV}$	
		$\Gamma_{\eta_c}(2S) = (11.3^{+3.2}_{-2.9})\text{MeV}$		$\Gamma_{\psi(2S)} = (294 \pm 8)\text{keV}$	

$$= i f_V m_V \left[- \left(m_\psi + m_{D_{(s)}} \right) A_1^{\psi D_{(s)}} \left(m_V^2 \right) \right.$$
$$\left. \times \pm \frac{2 m_\psi p_c}{m_\psi + m_D} V^{\psi D_{(s)}} \left(m_V^2 \right) \right]. \tag{46}$$

3 Numerical results and discussions

3.1 Transition form factors

The input parameters, including the masses of the initial and the final mesons, the CKM matrix elements, the shape parameters fitted by the decay constants, the full widths of the initial mesons, and so on are listed in Table 1. It is noted that the decay constant of charmonium $\eta_c(2S)$ is calculated as following formula [37]

$$f_{\eta_c(2S)} = \sqrt{\frac{81 m_{\eta_c(2S)} \Gamma_{\eta_c(2S) \to \gamma\gamma}}{64 \pi \alpha_{em}^2}}, \tag{47}$$

where $\Gamma_{\eta_c(2S)} \to \gamma\gamma = (1.3 \pm 0.6)$ keV is taken from the CLEO measurement [38]. Then one can obtain $f_{\eta_c(2S)} = (189^{+40}_{-50})$ MeV with smaller uncertainty compared with $f_{\eta_c(2S)} = (243^{+79}_{-111})$ MeV [29]. As to the decay constant of $\psi(2S)$, it is estimated from the relation $\frac{f_{\psi(2S)}}{f_{J/\psi}} = \frac{f_{\eta_c(2S)}}{f_{\eta_c}}$ [39] and given as $f_{\psi(2S)} = (210^{+43}_{-52})$ MeV. Based on the input parameters from Table 1, one can obtain the numerical results of the transition form factors at $q^2 = 0$ shown in Table 2.

All the computations are carried out within the $q^+ = 0$ reference frame, where the form factors can only be obtained at spacelike momentum transfers $q^2 = -q_\perp^2 \le 0$. It is needed to know the form factors in the timelike region for the physical decay processes. Here we use the following double-pole approximation to parametrize the form factors in the space-

like region and then extend to the timelike region,

$$F \left(q^2 \right) = \frac{F(0)}{1 - a q^2/m^2 + b q^4/m^4}, \tag{48}$$

where m represents the initial meson mass and $F(q^2)$ denotes the different form factors F_1, F_0, V, A_0, A_1 and A_2. The values of a and b can be obtained by performing a 3-parameter fit to the form factors in the range $-10 \text{GeV}^2 \le q^2 \le 0$, which are collected in Table 2. The uncertainties arise from the decay constants of the initial charmonia ($\eta_c(1S, 2S)$, $\psi(1S, 2S)$) and the final charmed mesons (D, D_s).

In Table 3, we compare the values of form factors at maximum recoil ($q^2 = 0$) with those obtained within the nonrelativistic quantum chromodynamics (NRQCD) [5], the BSW model [16] and the QCDSR [18]. It is found that our predictions for the form factors of the transitions $\eta_c \to D_{(s)}$, $J/\psi \to D_{(s)}$ are comparable with those given in the NRQCD and the BSW model with the parameter $\omega = 0.5$ GeV. Certainly, our results are also consistent with the previous CLFQM calculations [17] within errors. While those form factors predicted in the QCDSR [18] are much smaller than other theoretical predictions. As to the form factors of the $\eta_c(2S) \to D_{(s)}$, $\psi(2S) \to D_{(s)}$ transitions, only the theoretical results from the NRQCD approach are available, there exist obvious differences for some of values between these two approaches.

We plot the q^2-dependences of the $\eta_c(1S, 2S) \to D_{(s)}$ and $\psi(1S, 2S) \to D_{(s)}$ transition form factors shown in Fig. 2. It is very different for the q^2-dependences of the form factors $F_0(q^2)$ between the transitions $\eta_c(1S) \to D_{(s)}$ and $\eta_c(2S) \to D_{(s)}$. Among the form factors of the transition $J/\Psi(\psi(2S)) \to D_{(s)}$, $V^{J/\Psi D_{(s)}}(V^{\psi(2S)D_{(s)}})$ is the most sensitive to the q^2 variation compared with other three form factors.

Table 2 Form factors of the transitions $\eta_c(1S, 2S) \to D_{(s)}$, $\psi(1S, 2S) \to D_{(s)}$ in the CLFQM. The uncertainties are from the decay constants of initial and final state mesons

	$\eta_c \to D$			$J/\psi \to D$		
	F_1	F_0	V	A_0	A_1	A_2
$F(0)$	$0.73^{+0.00+0.03}_{-0.00-0.04}$	$0.73^{+0.00+0.03}_{-0.00-0.04}$	$1.73^{+0.01+0.03}_{-0.02-0.05}$	$0.45^{+0.02+0.02}_{-0.02-0.01}$	$0.53^{+0.01+0.00}_{-0.01-0.00}$	$0.13^{+0.06+0.07}_{-0.06-0.07}$
$F(q^2_{max})$	$0.75^{+0.00+0.03}_{-0.00-0.04}$	$0.59^{+0.00+0.03}_{-0.00-0.04}$	$1.38^{+0.01+0.01}_{-0.02-0.04}$	$0.45^{+0.02+0.01}_{-0.02-0.00}$	$0.54^{+0.01+0.01}_{-0.01-0.00}$	$0.11^{+0.06+0.07}_{-0.05-0.06}$
a	$0.41^{+0.01+0.05}_{-0.01-0.07}$	$-1.07^{+0.10+0.38}_{-0.10-0.32}$	$-0.23^{+0.13+0.20}_{-0.14-0.25}$	$0.30^{+0.05+0.04}_{-0.06-0.00}$	$0.41^{+0.04+0.00}_{-0.05-0.03}$	$-1.08^{+0.50+0.60}_{-0.79-0.93}$
b	$1.40^{+0.05+0.30}_{-0.05-0.24}$	$4.85^{+0.37+1.77}_{-0.35-1.37}$	$8.74^{+0.87+1.78}_{-0.80-1.45}$	$2.07^{+0.22+0.74}_{-0.20-0.51}$	$2.16^{+0.30+0.72}_{-0.26-0.52}$	$1.98^{+0.23+0.57}_{-0.09-0.04}$

	$\eta_c \to D_s$			$J/\psi \to D_s$		
	F_1	F_0	V	A_0	A_1	A_2
$F(0)$	$0.82^{+0.00+0.02}_{-0.00-0.07}$	$0.82^{+0.00+0.02}_{-0.00-0.07}$	$1.81^{+0.00+0.04}_{-0.01-0.06}$	$0.49^{+0.02+0.07}_{-0.03-0.05}$	$0.59^{+0.02+0.02}_{-0.02-0.05}$	$0.08^{+0.01+0.06}_{-0.02-0.06}$
$F(q^2_{max})$	$0.86^{+0.00+0.03}_{-0.00-0.07}$	$0.75^{+0.00+0.06}_{-0.00-0.07}$	$1.69^{+0.00+0.00}_{-0.01-0.02}$	$0.50^{+0.02+0.06}_{-0.03-0.06}$	$0.61^{+0.02+0.02}_{-0.02-0.05}$	$0.06^{+0.01+0.06}_{-0.02-0.05}$
a	$0.49^{+0.01+0.10}_{-0.01-0.02}$	$-0.49^{+0.07+0.44}_{-0.08-0.32}$	$0.20^{+0.08+0.26}_{-0.08-0.48}$	$0.34^{+0.03+0.05}_{-0.04-0.20}$	$0.45^{+0.02+0.13}_{-0.03-0.00}$	$-1.59^{+0.65+0.44}_{-0.87-1.51}$
b	$0.88^{+0.03+0.06}_{-0.03-0.03}$	$2.49^{+0.22+2.01}_{-0.24-1.63}$	$5.60^{+0.48+3.43}_{-0.44-2.13}$	$1.23^{+0.12+1.38}_{-0.11-0.60}$	$1.29^{+0.15+1.34}_{-0.14-0.63}$	$1.58^{+0.32+1.00}_{-0.24-0.01}$

	$\eta_c(2S) \to D$			$\psi(2S) \to D$		
	F_1	F_0	V	A_0	A_1	A_2
$F(0)$	$0.36^{+0.02+0.03}_{-0.09-0.03}$	$0.36^{+0.02+0.03}_{-0.09-0.03}$	$0.83^{+0.16+0.07}_{-0.17-0.08}$	$0.31^{+0.04+0.02}_{-0.08-0.02}$	$0.31^{+0.00+0.00}_{-0.03-0.00}$	$0.32^{+0.16+0.09}_{-0.24-0.09}$
$F(q^2_{max})$	$0.37^{+0.00+0.03}_{-0.07-0.04}$	$0.39^{+0.02+0.02}_{-0.14-0.03}$	$0.61^{+0.05+0.06}_{-0.12-0.07}$	$0.28^{+0.04+0.01}_{-0.09-0.01}$	$0.30^{+0.03+0.02}_{-0.03-0.01}$	$0.19^{+0.08+0.01}_{-0.14-0.04}$
a	$0.72^{+0.57+0.07}_{-0.12-0.11}$	$0.77^{+0.21+0.03}_{-0.72-0.10}$	$0.68^{+0.10+0.14}_{-0.95-0.23}$	$0.62^{+0.31+0.01}_{-0.54-0.09}$	$0.65^{+0.09+0.01}_{-0.28-0.06}$	$-0.09^{+0.24+0.15}_{-0.11-0.33}$
b	$2.52^{+3.22+0.26}_{-1.59-0.25}$	$1.72^{+0.98+0.55}_{-0.55-0.41}$	$8.78^{+7.33+0.46}_{-4.23-0.47}$	$4.31^{+1.27+1.76}_{-0.92-1.19}$	$3.31^{+2.18+1.07}_{-1.13-0.77}$	$10.52^{+2.47+6.01}_{-3.73-4.02}$

	$\eta_c(2S) \to D_s$			$\psi(2S) \to D_s$		
	F_1	F_0	V	A_0	A_1	A_2
$F(0)$	$0.44^{+0.03+0.02}_{-0.05-0.07}$	$0.44^{+0.03+0.02}_{-0.05-0.07}$	$0.99^{+0.08+0.05}_{-0.12-0.16}$	$0.30^{+0.05+0.06}_{-0.06-0.07}$	$0.33^{+0.01+0.01}_{-0.04-0.03}$	$0.19^{+0.16+0.24}_{-0.19-0.20}$
$F(q^2_{max})$	$0.48^{+0.00+0.01}_{-0.07-0.08}$	$0.50^{+0.06+0.03}_{-0.06-0.10}$	$0.86^{+0.05+0.01}_{-0.06-0.13}$	$0.30^{+0.06+0.05}_{-0.07-0.08}$	$0.35^{+0.00+0.02}_{-0.04-0.03}$	$0.15^{+0.15+0.16}_{-0.15-0.15}$
a	$0.83^{+0.05+0.00}_{-0.34-0.15}$	$0.79^{+0.20+0.25}_{-0.05-0.33}$	$0.91^{+0.28+0.08}_{-0.64-0.32}$	$0.54^{+0.24+0.16}_{-0.39-0.48}$	$0.71^{+0.07+0.00}_{-0.17-0.23}$	$-0.39^{+0.79+0.48}_{-1.71-1.96}$
b	$1.87^{+1.57+0.61}_{-1.06-0.57}$	$1.00^{+1.95+1.09}_{-0.07-0.53}$	$7.45^{+4.87+1.33}_{-3.00-1.71}$	$2.32^{+0.70+1.63}_{-0.47-1.09}$	$1.99^{+1.14+1.93}_{-0.65-0.91}$	$4.21^{+1.04+3.71}_{-0.27-1.26}$

3.2 Semileptonic decays

The semileptonic decay of heavy flavor mesons offers a excellent platform for extraction of the Cabibbo–Kobayashi–Maskawa (CKM) matrix elements, which describe the CP-violating and flavor changing processes in the Standard Model. The form factors involving the dynamical information play an essential role in these semileptonic decays. Based on the form factors and the helicity amplitudes provided in the previous section, the branching ratios of the semileptonic $\eta_c(1S, 2S)$ and $\psi(1S, 2S)$ decays are presented in Table 4, where the uncertainties arise from the decay widths of initial charmonia, the decay constants of initial and final state mesons, respectively. Several remarks are in order

1. For these semileptonic $\eta_c(1S, 2S)$ and $\psi(1S, 2S)$ decays, their branching ratios are in the range $10^{-14} \sim 10^{-12}$ and $10^{-11} \sim 10^{-10}$, respectively. Some of these decays

might be detected by the future high-luminosity experiments, such as the Super Tau-Charm Factory (STCF), BESIII and LHC.

2. Our predictions for the branching ratios of the decays $J/\Psi \to D^-_{(s)}\ell^+\nu_\ell$ are consistent with those given in the BSW model [16]. Certainly, they are also agreement with the previous CLFQM estimates and the differences are mainly from the input parameters. While these results are some three or more times as large as those given by the BS approach [19], the CCQM [23] and the QCDSR [20]. Except the variations from the input parameters, the main reason is the distinct treatment of nonperturbative dynamics, which can to be clarified by the future accurate measurements. At present BESIII only gives some upper limits, which are still much larger than all the theoretical values.

3. The branching ratios of the decays $\eta_c(2S) \to D^-_{(s)}\ell^+\nu_\ell$ are larger than those of the decays $\eta_c \to D^-_{(s)}\ell^+\nu_\ell$. It

Table 3 Numerical values of the transition form factors at $q^2 = 0$, together with other theoretical results

Transition	Reference	$F_0(0)$	$V(0)$	$A_0(0)$	$A_1(0)$	$A_2(0)$
$\eta_c, J/\psi \to D$	This work	0.73	1.73	0.45	0.53	0.13
	[5]	0.85	1.76	0.85	0.72	–
	[16][a]	–	2.14	0.55	0.77	0.31
	[16][b]	–	2.21	0.54	0.80	0.47
	[2][c]	–	1.82	0.61	0.68	0.33
	[17]	–	1.6	0.68	0.68	0.18
	[18]	–	0.81	0.27	0.27	–
$\eta_c, J/\psi \to D_s$	This work	0.82	1.81	0.49	0.59	0.08
	[5]	0.90	1.55	0.90	0.81	–
	[16][a]	–	2.30	0.71	0.94	0.33
	[16][b]	–	2.36	0.69	0.96	0.51
	[2][c]	–	1.80	0.66	0.78	0.12
	[17]	–	1.8	0.68	0.68	0.13
	[18]	–	1.07	0.37	0.38	–
$\eta_c(2S), \psi(2S) \to D$	This work	0.36	0.83	0.31	0.31	0.32
	[5]	0.62	1.00	0.61	0.54	–
$\eta_c(2S), \psi(2S) \to D_s$	This work	0.44	0.99	0.30	0.33	0.19
	[5]	0.65	0.83	0.64	0.59	–

[a]The form factors are computed with flavor dependent parameter ω using the WSB model
[b]The form factors are computed with the QCD inspired parameter $\omega = m\alpha_s$ using in the WSB model
[c]The form factors are computed with the parameter $\omega = 0.5$ GeV using the WSB model

is contrary for the cases of the decays $\psi(1S, 2S) \to D_{(s)}^- \ell^+ \nu_\ell$, where $Br(\psi(2S) \to D_{(s)}^- \ell^+ \nu_\ell) < Br(J/\Psi \to D_{(s)}^- \ell^+ \nu_\ell)$. These are related with their total widths, $\Gamma_{\eta_c}(\Gamma_{\psi(2S)})$ is about 3 times as large as $\Gamma_{\eta_c(2S)}(\Gamma_{J/\Psi})$.

4. In order to cancel out a large part of the theoretical and experimental uncertainties, to check the lepton flavor universality (LFU) and to detect the effect of SU(3) symmetry breaking, it is helpful to consider the ratio $R \equiv \mathcal{B}r(\eta_c(\psi) \to D_s^- \ell^+ \nu_\ell)/\mathcal{B}r(\eta_c(\psi) \to D^- \ell^+ \nu_\ell)$, which should be equal to $|V_{cs}/V_{cd}|^2 \approx 19.46$ under the $SU(3)$ flavor symmetry limit. Their values in this work are listed as

$$R_{\eta_c}^e = \frac{\eta_c \to D_s^- e^+ \nu_e}{\eta_c \to D^- e^+ \nu_e} = 16.52 \pm 2.73,$$

$$R_{\eta_c(2S)}^e = \frac{\eta_c(2S) \to D_s^- e^+ \nu_e}{\eta_c(2S) \to D^- e^+ \nu_e} = 23.59 \pm 13.06,$$

$$R_{\eta_c}^\mu = \frac{\eta_c \to D_s^- \mu^+ \nu_\mu}{\eta_c \to D^- \mu^+ \nu_\mu} = 16.43 \pm 3.27,$$

$$R_{\eta_c(2S)}^\mu = \frac{\eta_c(2S) \to D_s^- \mu^+ \nu_\mu}{\eta_c(2S) \to D^- \mu^+ \nu_\mu} = 23.54 \pm 13.07,$$

$$R_{J/\psi}^e = \frac{J/\psi \to D_s^- e^+ \nu_e}{J/\psi \to D^- e^+ \nu_e} = 16.74 \pm 2.37,$$

$$R_{\psi(2S)}^e = \frac{\psi(2S) \to D_s^- e^+ \nu_e}{\psi(2S) \to D^- e^+ \nu_e} = 20.87 \pm 4.09,$$

$$R_{J/\psi}^\mu = \frac{J/\psi \to D_s^- \mu^+ \nu_\mu}{J/\psi \to D^- \mu^+ \nu_\mu} = 16.59 \pm 2.36,$$

$$R_{\psi(2S)}^\mu = \frac{\psi(2S) \to D_s^- \mu^+ \nu_\mu}{\psi(2S) \to D^- \mu^+ \nu_\mu} = 20.71 \pm 3.62. \quad (49)$$

It is obviously there exist some effects of $SU(3)$ symmetry breaking in these semi-leptonic decays. The ratios $R_{J/\psi}^{e,\mu}$ are consistent with that given in Ref. [19], where $R_{J/\psi}^\ell = 18.1$. Certainly, the values of these ratios are in agreement with the predictions under the $SU(3)$ flavor symmetry limit within errors. The large uncertainties from the ratios $R_{\eta_c(2S)}^\ell$ are mainly induced by the decay width of $\eta_c(2S)$, $\Gamma_{\eta_c(2S)} = (11.3_{-2.9}^{+3.2})$ MeV.

3.3 Physical observables

In order to study the impact of lepton mass and provide a more detailed physical picture for the semileptonic decays, we also define other two physical observables on the basis of form factors and helicity formalism, that is the forward–backward asymmetry A_{FB} and the longitudinal polarization fraction f_L. The results of these two physical observables are listed in Tables 5 and 6, respectively. We find that the ratios of the forward–backward asymmetries A_{FB}^μ/A_{FB}^e between the semileptonic decays $\eta_c \to D_{(s)}^- \mu^+ \nu_\mu$ and $\eta_c \to D_{(s)}^- e^+ \nu_e$ are about $1.9(1.8) \times 10^4$ for $\eta_c(1S)$ and
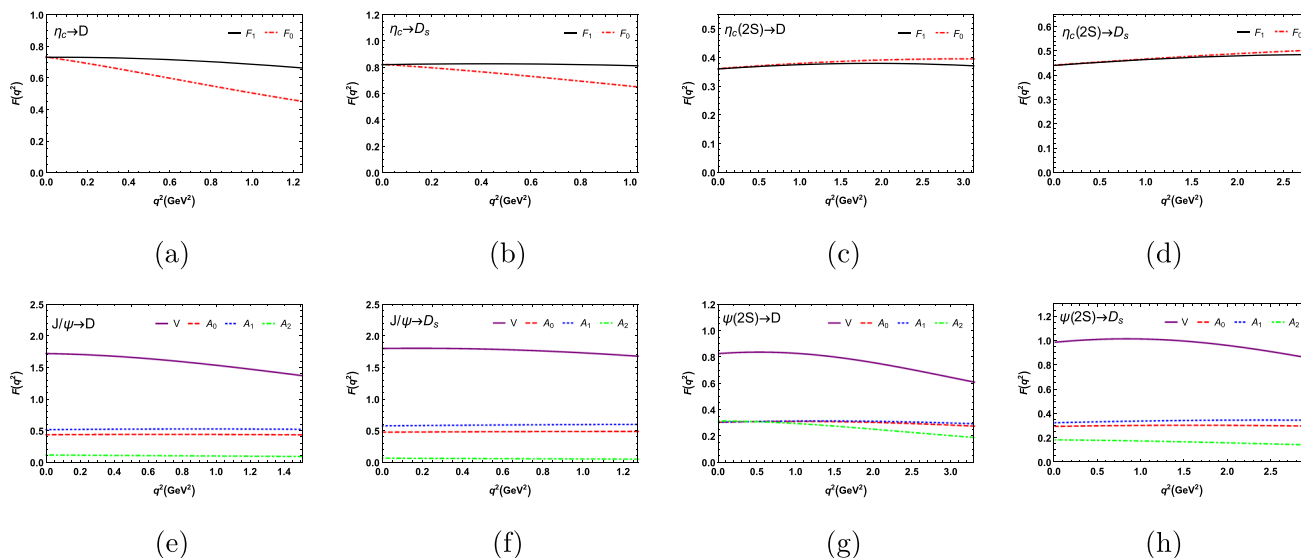
Fig. 2 Form factors $F_1(q^2)$ and $F_0(q^2)$ for the transitions $\eta_c(1S, 2S) \to D_{(s)}$ and form factors $V(q^2)$, $A_0(q^2)$, $A_1(q^2)$ and $A_2(q^2)$ for the transitions $\psi(1S, 2S) \to D_{(s)}$, respectively

Table 4 The branching ratios of the semileptonic $\eta_c(1S, 2S)$ and $\psi(1S, 2S)$ decays

	$10^{-14} \times \mathcal{B}r(\eta_c \to D^- e^+ \nu_e)$	$10^{-14} \times \mathcal{B}r(\eta_c \to D^- \mu^+ \nu_\mu)$	$10^{-13} \times \mathcal{B}r(\eta_c \to D_s^- e^+ \nu_e)$	$10^{-13} \times \mathcal{B}r(\eta_c \to D_s^- \mu^+ \nu_\mu)$
This work	$5.43^{+0.12+0.00+0.47}_{-0.12-0.00-0.60}$	$5.15^{+0.12+0.00+0.45}_{-0.11-0.00-0.57}$	$8.97^{+0.20+0.01+0.51}_{-0.19-0.01-1.48}$	$8.46^{+0.19+0.01+0.50}_{-0.18-0.01-1.40}$
	$10^{-11} \times \mathcal{B}r(J/\psi \to D^- e^+ \nu_e)$	$10^{-11} \times \mathcal{B}r(J/\psi \to D^- \mu^+ \nu_\mu)$	$10^{-10} \times \mathcal{B}r(J/\psi \to D_s^- e^+ \nu_e)$	$10^{-10} \times \mathcal{B}r(J/\psi \to D_s^- \mu^+ \nu_\mu)$
This work	$6.10^{+0.11+0.10+0.14}_{-0.11-0.12-0.19}$	$5.78^{+0.11+0.11+0.16}_{-0.10-0.13-0.11}$	$10.21^{+0.19+0.66+0.56}_{-0.18-0.61-1.41}$	$9.59^{+0.18+0.62+0.63}_{-0.17-0.58-1.34}$
QCDSR [20]	0.73	0.71	1.8	1.7
LFQM [17]	$5.1 \sim 5.7$	$4.7 \sim 5.5$	$5.3 \sim 5.8$	$5.5 \sim 5.7$
BSW [16]	6.0	5.8	10.4	9.93
CCQM [23]	1.71	1.66	3.3	3.2
BS [19]	2.03	1.98	3.67	3.54
Exp. [13–15]	$< 7.1 \times 10^3$	$< 5.6 \times 10^4$	$< 1.3 \times 10^4$	–
	$10^{-13} \times \mathcal{B}r(\eta_c(2S) \to D^- e^+ \nu_e)$	$10^{-13} \times \mathcal{B}r(\eta_c(2S) \to D^- \mu^+ \nu_\mu)$	$10^{-12} \times \mathcal{B}r(\eta_c(2S) \to D_s^- e^+ \nu_e)$	$10^{-12} \times \mathcal{B}r(\eta_c(2S) \to D_s^- \mu^+ \nu_\mu)$
This work	$3.12^{+1.08+0.47+0.56}_{-0.69-1.35-0.53}$	$3.08^{+1.06+0.47+0.56}_{-0.68-1.34-0.52}$	$7.36^{+2.54+0.93+0.62}_{-1.62-1.75-2.22}$	$7.25^{+2.50+0.91+0.60}_{-1.60-1.73-2.19}$
	$10^{-11} \times \mathcal{B}r(\psi(2S) \to D^- e^+ \nu_e)$	$10^{-11} \times \mathcal{B}r(\psi(2S) \to D^- \mu^+ \nu_\mu)$	$10^{-10} \times \mathcal{B}r(\psi(2S) \to D_s^- e^+ \nu_e)$	$10^{-10} \times \mathcal{B}r(\psi(2S) \to D_s^- \mu^+ \nu_\mu)$
This work	$3.45^{+0.10+0.49+0.23}_{-0.09-0.20-0.25}$	$3.39^{+0.09+0.11+0.21}_{-0.09-0.35-0.23}$	$7.20^{+0.20+0.97+0.60}_{-0.19-0.44-0.92}$	$7.02^{+0.20+0.99+0.65}_{-0.19-0.38-0.83}$

Table 5 The forward–backward asymmetry A_{FB}

Channel	$\eta_c \to D^- e^+ \nu_e$	$\eta_c \to D^- \mu^+ \nu_\mu$	$\eta_c \to D_s^- e^+ \nu_e$	$\eta_c \to D_s^- \mu^+ \nu_\mu$
A_{FB}	$(4.21^{+0.09+0.00+0.37}_{-0.09-0.00-0.46}) \times 10^{-6}$	$0.080^{+0.002+0.000+0.007}_{-0.002-0.000-0.009}$	$(5.08^{+0.11+0.00+0.28}_{-0.11-0.00-0.84}) \times 10^{-6}$	$0.091^{+0.002+0.000+0.006}_{-0.002-0.000-0.015}$
Channel	$J/\psi \to D^- e^+ \nu_e$	$J/\psi \to D^- \mu^+ \nu_\mu$	$J/\psi \to D_s^- e^+ \nu_e$	$J/\psi \to D_s^- \mu^+ \nu_\mu$
A_{FB}	$-0.23^{+0.00+0.01+0.01}_{-0.00-0.00-0.00}$	$-0.23^{+0.00+0.01+0.01}_{-0.00-0.01-0.00}$	$-0.21^{+0.00+0.01+0.03}_{-0.00-0.01-0.01}$	$-0.22^{+0.00+0.01+0.03}_{-0.00-0.01-0.01}$
Channel	$\eta_c(2S) \to D^- e^+ \nu_e$	$\eta_c(2S) \to D^- \mu^+ \nu_\mu$	$\eta_c(2S) \to D_s^- e^+ \nu_e$	$\eta_c(2S) \to D_s^- \mu^+ \nu_\mu$
A_{FB}	$(1.69^{+0.58+0.21+0.30}_{-0.37-0.76-0.28}) \times 10^{-6}$	$0.045^{+0.016+0.006+0.008}_{-0.010-0.021-0.007}$	$(1.86^{+0.64+0.27+0.19}_{-0.41-0.41-0.56}) \times 10^{-6}$	$0.048^{+0.017+0.007+0.005}_{-0.011-0.011-0.015}$
Channel	$\psi(2S) \to D^- e^+ \nu_e$	$\psi(2S) \to D^- \mu^+ \nu_\mu$	$\psi(2S) \to D_s^- e^+ \nu_e$	$\psi(2S) \to D_s^- \mu^+ \nu_\mu$
A_{FB}	$-0.28^{+0.01+0.09+0.03}_{-0.01-0.02-0.02}$	$-0.28^{+0.01+0.09+0.03}_{-0.01-0.02-0.02}$	$-0.27^{+0.01+0.07+0.07}_{-0.01-0.02-0.01}$	$-0.27^{+0.01+0.07+0.07}_{-0.01-0.02-0.01}$

Table 6 The partial branching ratios and the longitudinal polarization fractions f_L for the decays $\psi(1S, 2S) \to D_{(s)}^- \ell^+ \nu_\ell$ in Region 1 and Region 2

Observables	Region 1	Region 2	Total
$Br(J/\psi \to D^- e^+ \nu_e)$	3.54×10^{-11}	2.55×10^{-11}	6.10×10^{-11}
$f_L(J/\psi \to D^- e^+ \nu_e)$	0.68	0.42	$0.57^{+0.01+0.00+0.03}_{-0.01-0.00-0.03}$
$Br(J/\psi \to D_s^- e^+ \nu_e)$	5.83×10^{-10}	4.38×10^{-10}	10.21×10^{-10}
$f_L(J/\psi \to D_s^- e^+ \nu_e)$	0.70	0.43	$0.58^{+0.01+0.04+0.03}_{-0.01-0.03-0.08}$

Observables	Region 1	Region 2	Total
$Br(J/\psi \to D^- \mu^+ \nu_\mu)$	3.31×10^{-11}	2.46×10^{-11}	5.78×10^{-11}
$f_L(J/\psi \to D^- \mu^+ \nu_\mu)$	0.67	0.42	$0.56^{+0.00+0.00+0.03}_{-0.01-0.01-0.02}$
$Br(J/\psi \to D_s^- \mu^+ \nu_\mu)$	5.39×10^{-10}	4.20×10^{-10}	9.59×10^{-10}
$f_L(J/\psi \to D_s^- \mu^+ \nu_\mu)$	0.68	0.43	$0.57^{+0.01+0.04+0.03}_{-0.01-0.03-0.08}$

Observables	Region 1	Region 2	Total
$Br(\psi(2S) \to D^- e^+ \nu_e)$	1.91×10^{-11}	1.54×10^{-11}	3.45×10^{-11}
$f_L(\psi(2S) \to D^- e^+ \nu_e)$	0.60	0.40	$0.51^{+0.01+0.07+0.08}_{-0.01-0.14-0.08}$
$Br(\psi(2S) \to D_s^- e^+ \nu_e)$	4.06×10^{-10}	3.14×10^{-10}	7.20×10^{-10}
$f_L(\psi(2S) \to D_s^- e^+ \nu_e)$	0.65	0.41	$0.54^{+0.02+0.02+0.02}_{-0.01-0.08-0.14}$

Observables	Region 1	Region 2	Total
$Br(\psi(2S) \to D^- \mu^+ \nu_\mu)$	1.88×10^{-11}	1.51×10^{-11}	3.39×10^{-11}
$f_L(\psi(2S) \to D^- \mu^+ \nu_\mu)$	0.60	0.40	$0.51^{+0.01+0.05+0.08}_{-0.01-0.13-0.07}$
$Br(\psi(2S) \to D_s^- \mu^+ \nu_\mu)$	3.94×10^{-10}	3.08×10^{-10}	7.02×10^{-10}
$f_L(\psi(2S) \to D_s^- \mu^+ \nu_\mu)$	0.64	0.41	$0.54^{+0.02+0.03+0.01}_{-0.01-0.08-0.13}$

$2.7(2.6) \times 10^4$ for $\eta_c(2S)$, respectively. The reason is that the forward–backward asymmetries A_{FB} for the decays $\eta_c(1S, 2S) \to D_{(s)}^- \ell^+ \nu_\ell$ are proportional to the square of the lepton mass. Undoubtedly, the effect of lepton mass can be well checked in such decay mode with a pseudoscalar meson involved in the final states. It is similar to the decays $B_c \to \eta_c(1S, 2S, 3S)\ell^+\nu_\ell$ [40]. While for the decays $\psi(1S, 2S) \to D_{(s)}^-\ell^+\nu_\ell$, the values of the forward–backward asymmetries A_{FB}^μ and A_{FB}^e are almost equal to each other. It is noted that the dominant contributions to the A_{FB} for the transitions $\psi(1S, 2S) \to D_{(s)}$ arise from the terms proportional to $(H_{V,+}^2 - H_{V,-}^2)$ in Eq. (24).

In Table 6, we can clearly find that the longitudinal polarization fractions f_L between the decays $\psi(1S, 2S) \to D_{(s)}^- e^+ \nu_e$ and $\psi(1S, 2S) \to D_{(s)}^- \mu^+ \nu_\mu$ are very close to each other

$$f_L(\psi(1S, 2S) \to D_{(s)}^- e^+ \nu_e) \sim f_L(\psi(1S, 2S) \to D_{(s)}^- \mu^+ \nu_\mu), \tag{50}$$

which reflects the lepton flavor universality (LFU). In order to investigate the dependences of the polarizations on the different q^2, we calculate the longitudinal polarization fractions by dividing the full energy region into two regions for each decay. Region 1 is defined as $m_\ell^2 < q^2 < \frac{(m_{\psi(nS)} - m_{D_{(s)}})^2 + m_\ell^2}{2}$ and Region 2 is $\frac{(m_{\psi(nS)} - m_{D_{(s)}})^2 + m_\ell^2}{2} < q^2 < (m_{\psi(nS)} - m_{D_{(s)}})^2$ with $n = 1, 2$. Interestingly, for the decays $\psi(1S, 2S) \to D_{(s)}^-\ell^+\nu_\ell$ the longitudinal (transverse) polarization is dominant in Region 1 (Region 2). While these two kinds of polarizations are comparable in the entire physical region. These results can be tested by the future high-luminosity experiments.

In Figs. 3 and 4, we also display the q^2-dependences of differential decay rates $d\Gamma_{(L)}/dq^2$ and forward–backward asymmetries A_{FB}, respectively. It can be observed that the values of $d\Gamma_{(L)}/dq^2$ and A_{FB} coincide with 0 at the zero recoil point ($q^2 = q_{max}^2$) since the coefficient $\sqrt{\lambda(q^2)} = \sqrt{\lambda(m_{\eta_c, J/\psi}^2, m_{D_s}^2, q^2)}$ shown in Eqs. (17–24) at the same zero recoil point being equal to 0. The lepton mass effects can be obviously observed from Fig. 4a–d.

3.4 Nonleptonic decays

The decays rates of the charmonium weak decays $\eta_c(1S, 2S) \to D_{(s)}M$ and $\psi(1S, 2S) \to D_{(s)}M$ with M standing for a pseudoscalar meson (P) or a vector meson (V) can be written as

$$Br\left(\eta_c(1S, 2S) \to D_{(s)}M\right) = \frac{p_{cm}}{4\pi m_{\eta_c(1S,2S)}^2 \Gamma_{\eta_c(1S,2S)}} \left|\mathcal{A}\left(\eta_c(1S, 2S) \to D_{(s)}M\right)\right|^2, \tag{51}$$
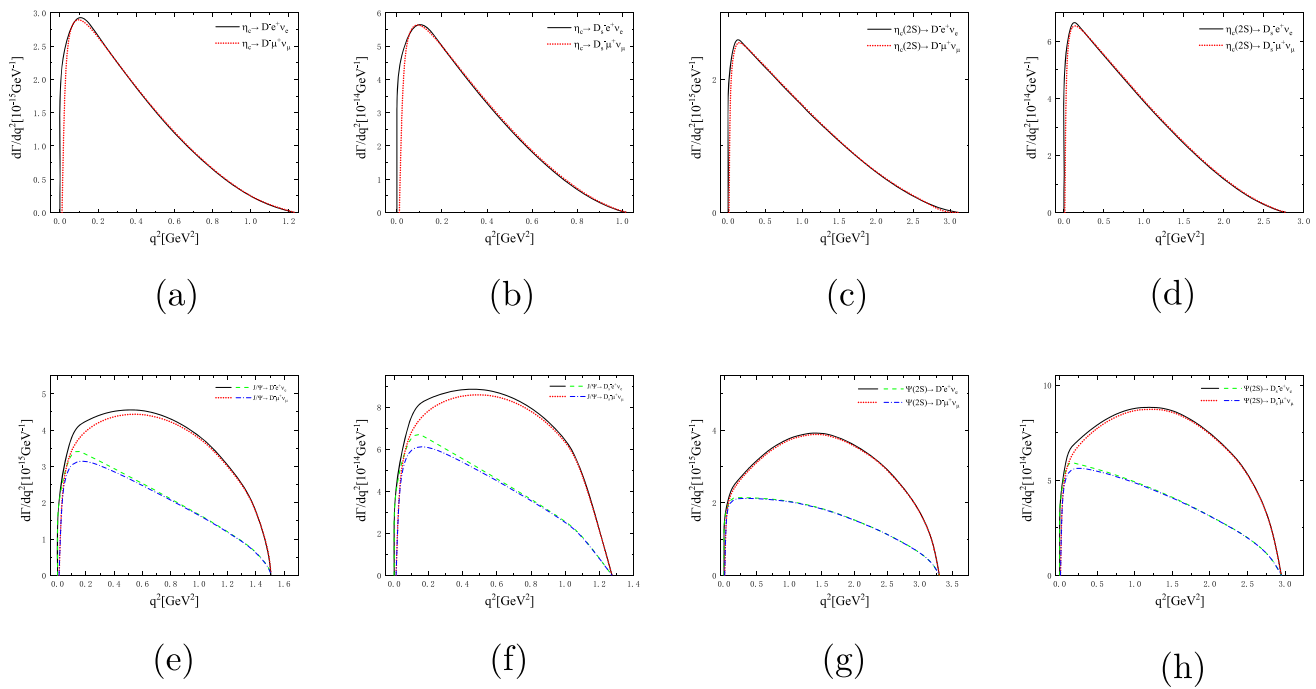
Fig. 3 The theoretical predictions for the q^2 dependences of the differential decay rates $d\Gamma/dq^2$ and $d\Gamma^L/dq^2$
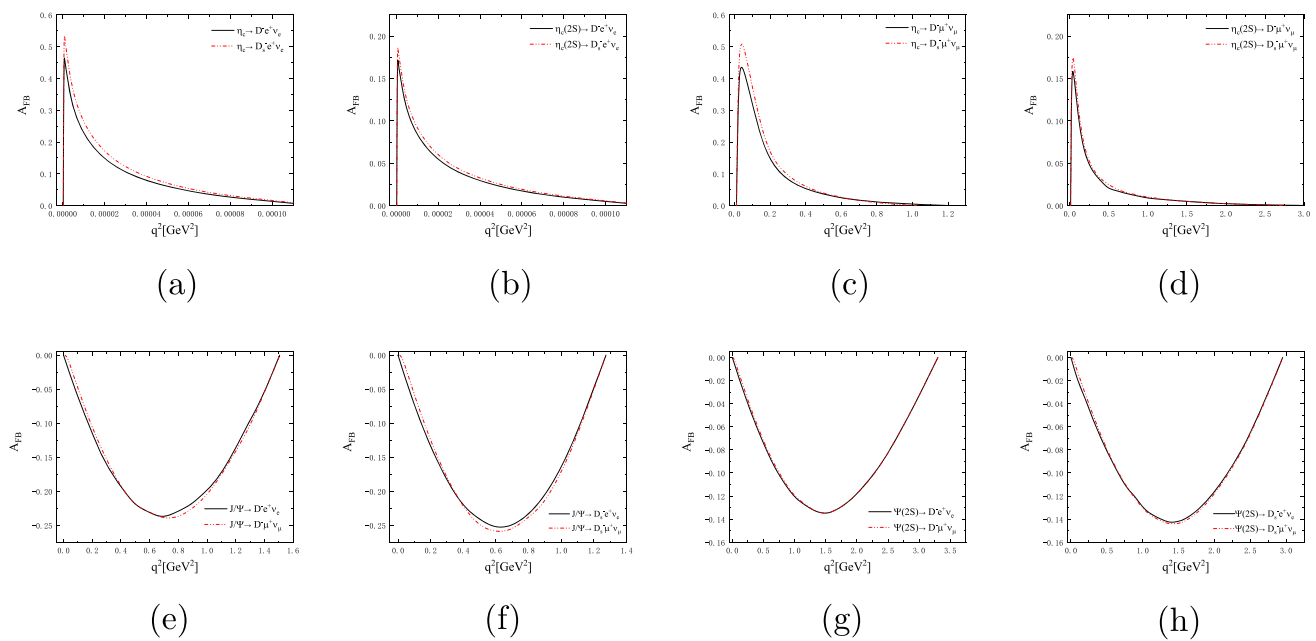

Fig. 4 The theoretical predictions for the q^2 dependences of the forward–backward asymmetries A_{FB}

$$\mathcal{B}r\left(\psi(1S, 2S) \to D_{(s)}M\right) = \frac{p_{\text{cm}}}{12\pi m_{\psi(1S,2S)}^2 \Gamma_{\psi(1S,2S)}}$$
$$|A(\psi(1S, 2S) \to D_{(s)}M)|^2. \quad (52)$$

where p_{cm} represents the three-momentum of the final meson $D_{(s)}$ in the rest frame of $\eta_c(1S, 2S)$ and $\psi(1S, 2S)$.

In Tables 7 and 8, we list the branching ratios of the non-leptonic decays $\eta_c(1 S, 2 S) \to D_{(s)}M$ and $\psi(1 S, 2 S) \to$

$D_{(s)}M$, including the values obtained from Refs. [1,5,6,16–18,20,21,21,22] and BESIII collaboration [11,12] for comparison, where the uncertainties of our results arise from the full widths of the charmonia $\eta_c(1S, 2S)$, $\psi(1S, 2S)$, the decay constants of the initial and final state mesons, respectively. The decay modes considered here are dominated by the color-favored factorizable contributions and insensitive

Table 7 Branching ratios of the nonleptonic ground charmonium state (J/ψ, η_c) decays

	$10^{-12} \times \mathcal{B}r(\eta_c \to D_s^- \pi^+)$	$10^{-13} \times \mathcal{B}r(\eta_c \to D_s^- K^+)$	$10^{-13} \times \mathcal{B}r(\eta_c \to D^- \pi^+)$	$10^{-14} \times \mathcal{B}r(\eta_c \to D^- K^+)$
This work	$6.65^{+0.15+0.01+0.32}_{-0.14-0.01-0.10}$	$4.22^{+0.09+0.00+0.35}_{-0.09-0.00-0.79}$	$3.34^{+0.07+0.01+0.28}_{-0.07-0.02-0.33}$	$2.33^{+0.05+0.01+0.21}_{-0.05-0.01-0.24}$
[5]	7.35	4.97	4.39	3.04
	$10^{-12} \times \mathcal{B}r(\eta_c \to D_s^- \rho^+)$	$10^{-13} \times \mathcal{B}r(\eta_c \to D_s^- K^{*+})$	$10^{-13} \times \mathcal{B}r(\eta_c \to D^- \rho^+)$	$10^{-14} \times \mathcal{B}r(\eta_c \to D^- K^{*+})$
This work	$6.62^{+0.15+0.03+0.69}_{-0.14-0.03-1.34}$	$3.31^{+0.07+0.02+0.40}_{-0.07-0.02-0.72}$	$3.01^{+0.07+0.00+0.33}_{-0.06-0.00-0.37}$	$1.68^{+0.04+0.00+0.20}_{-0.04-0.00-0.22}$
[5]	5.28	1.18	4.32	1.38
	$10^{-10} \times \mathcal{B}r(J/\psi \to D_s^- \pi^+)$	$10^{-11} \times \mathcal{B}r(J/\psi \to D_s^- K^+)$	$10^{-11} \times \mathcal{B}r(J/\psi \to D^- \pi^+)$	$10^{-12} \times \mathcal{B}r(J/\psi \to D^- K^+)$
This work	$3.64^{+0.06+0.34+0.78}_{-0.06-0.38-0.96}$	$2.02^{+0.04+0.18+0.36}_{-0.04-0.20-0.48}$	$1.90^{+0.04+0.17+0.11}_{-0.03-0.19-0.14}$	$1.16^{+0.02+0.03+0.13}_{-0.02-0.02-0.18}$
[5]	10.9	6.18	6.37	3.79
[6]	4.30	2.69	2.09	1.34
[16][a]	3.32	2.4	1.5	1.2
[17]	2.5	–	–	50
[18]	2.0	1.6	0.80	36
[1][b]	8.74	5.5	5.5	–
[21]	4.10	2.32	2.21	1.31
BES [11]	$< 1.4 \times 10^6$	–	$< 7.5 \times 10^6$	–
	$10^{-9} \times \mathcal{B}r(J/\psi \to D_s^- \rho^+)$	$10^{-10} \times \mathcal{B}r(J/\psi \to D_s^- K^{*+})$	$10^{-10} \times \mathcal{B}r(J/\psi \to D^- \rho^+)$	$10^{-12} \times \mathcal{B}r(J/\psi \to D^- K^{*+})$
This work	$2.95^{+0.06+0.11+0.15}_{-0.05-0.14-0.19}$	$1.42^{+0.03+0.06+0.07}_{-0.03-0.07-0.10}$	$1.70^{+0.03+0.03+0.07}_{-0.03-0.05-0.10}$	$8.59^{+0.16+0.20+0.42}_{-0.15-0.29-0.60}$
[5]	3.82	2.00	2.12	11.4
[16][a]	1.77	0.97	0.72	4.2
[17]	2.8	–	–	550
[18]	1.26	0.82	0.42	154
[1][b]	3.63	2.12	2.20	–
[21]	2.21	1.22	1.09	6.14
[22]	3.33	1.86	1.32	8.0
BES [12]	$< 1.3 \times 10^4$	–	–	–

[a] The branching ratios are computed with the average transverse quark momentum $\omega = 0.4$ GeV under the WSB model
[b] The branching ratios are computed with the average transverse quark momentum $\omega = 0.5$ GeV under the WSB model

Table 8 Branching ratios of the nonleptonic radially excited charmonium ($\eta_c(2S)$, $\psi(2S)$) decays

	$10^{-11} \times \mathcal{B}r(\eta_c(2S) \to D_s^- \pi^+)$	$10^{-12} \times \mathcal{B}r(\eta_c(2S) \to D_s^- K^+)$	$10^{-13} \times \mathcal{B}r(\eta_c(2S) \to D^- \pi^+)$	$10^{-14} \times \mathcal{B}r(\eta_c(2S) \to D^- K^+)$
This work	$1.92^{+0.66+0.24+0.18}_{-0.42-0.44-0.54}$	$1.29^{+0.45+0.13+0.17}_{-0.29-0.33-0.40}$	$7.67^{+2.65+0.78+1.24}_{-1.69-3.29-1.40}$	$5.08^{+1.75+0.63+0.90}_{-1.12-2.24-0.97}$
[5]	3.90	2.87	21.3	15.8
	$10^{-11} \times \mathcal{B}r(\eta_c(2S) \to D_s^- \rho^+)$	$10^{-13} \times \mathcal{B}r(\eta_c(2S) \to D_s^- K^{*+})$	$10^{-13} \times \mathcal{B}r(\eta_c(2S) \to D^- \rho^+)$	$10^{-14} \times \mathcal{B}r(\eta_c(2S) \to D^- K^{*+})$
This work	$1.92^{+0.66+0.10+0.67}_{-0.42-0.11-1.16}$	$7.05^{+2.43+1.12+1.21}_{-1.56-1.15-2.13}$	$3.93^{+1.36+0.08+0.68}_{-0.87-0.33-0.71}$	$2.54^{+0.88+0.38+0.44}_{-0.56-0.78-0.45}$
[5]	7.24	34.7	41.3	20.2
	$10^{-10} \times \mathcal{B}r(\psi(2S) \to D_s^- \pi^+)$	$10^{-12} \times \mathcal{B}r(\psi(2S) \to D_s^- K^+)$	$10^{-12} \times \mathcal{B}r(\psi(2S) \to D^- \pi^+)$	$10^{-13} \times \mathcal{B}r(\psi(2S) \to D^- K^+)$
This work	$1.23^{+0.03+0.08+0.59}_{-0.03-0.18-0.51}$	$8.20^{+0.22+2.62+3.34}_{-0.22-3.50-3.20}$	$7.58^{+0.22+2.32+1.06}_{-0.20-3.40-1.12}$	$4.96^{+0.14+1.42+0.56}_{-0.14-2.14-0.64}$
[5]	5.07	34.3	27.6	19
	$10^{-9} \times \mathcal{B}r(\psi(2S) \to D_s^- \rho^+)$	$10^{-11} \times \mathcal{B}r(\psi(2S) \to D_s^- K^{*+})$	$10^{-11} \times \mathcal{B}r(\psi(2S) \to D^- \rho^+)$	$10^{-12} \times \mathcal{B}r(\psi(2S) \to D^- K^{*+})$
This work	$1.22^{+0.03+0.01+0.41}_{-0.03-0.10-0.19}$	$7.31^{+0.20+0.06+0.42}_{-0.19-0.21-0.13}$	$5.55^{+0.16+0.59+0.52}_{-0.15-0.82-0.58}$	$3.31^{+0.09+0.33+0.34}_{-0.09-0.49-0.37}$
[5]	1.67	9.6	8.99	5.2

to the nonfactorizable contributions. Therefore, even with different phenomenological models, the branching ratios for a given decay process of $\eta_c(1S, 2S) \to D_{(s)}M$ and $\psi(1S, 2S) \to D_{(s)}M$ have the same order of magnitude in many cases. Numerically, we adopt the Wilson coefficient $a_1 = 1.26$. The following are some comments:

1. The branching ratios for the weak decays $\eta_c(2S) \to D_{(s)}M$ are approximately $1.5 \sim 3$ times larger than those

Table 9 The units of the branching ratios of the Cabbibo-favored and Cabbibo-suppressed decay channels

Cabbibo-favored decays	Order of magnitude	Cabbibo-suppressed decays	Order of magnitude
$\eta_c(1S, 2S) \to D_s^- \pi^+$	$(10^{-12} - 10^{-11})$	$\eta_c(1S, 2S) \to D^- K^+$	10^{-14}
$\psi(1S, 2S) \to D_s^- \pi^+$	$(10^{-11} - 10^{-10})$	$\psi(1S, 2S) \to D^- K^+$	10^{-13}
$\eta_c(1S, 2S) \to D_s^- \rho^+$	$(10^{-12} - 10^{-11})$	$\eta_c(1S, 2S) \to D^- K^{*+}$	10^{-14}
$\psi(1S, 2S) \to D_s^- \rho^+$	10^{-9}	$\psi(1S, 2S) \to D^- K^{*+}$	10^{-12}

for the corresponding decays $\eta_c \to D_{(s)}M$ due to the smaller decay width of $\eta_c(2S)$, $\Gamma_{\eta_c(2S)} = (11.3^{+3.2}_{-2.9})$ MeV compared to $\Gamma_{\eta_c} = (32.0 \pm 0.7)$ MeV for η_c meson, and the larger phase space for $\eta_c(2S)$. It is contrary for the cases of weak decays between $\psi(2S) \to D_{(s)}M$ and $J/\Psi \to D_{(s)}M$, where the branching ratios of the latter are about $2 \sim 3$ times larger than those of the former, because the decay width of J/ψ, $\Gamma_{J/\psi} = (92.6 \pm 1.7)$ keV is only about one-third of that for $\psi(2S)$, $\Gamma_{\psi(2S)} = (294 \pm 8)$ keV. These numerical relations are similar with those given by the NRQCD [5] for the J/Ψ and $\psi(2S)$ decays, while are different for the η_c and $\eta_c(2S)$ decays, where the differences are five times even more large.

2. It is worth mentioning that the branching ratios of the decays $\eta_c \to D_{(s)}M$ are in agreement with the results obtained the NRQCD approach [5], while there exists about $2 \sim 3$ times even more large difference for those of the decays $\eta_c(2S) \to D_{(s)}M$. For the J/Ψ weak decays, the branching ratios of the channels $J/\psi \to D_{(s)}V$ are consistent with most of other theoretical results, such as the NRQCD [5], the BSW model with the parameter $\omega = 0.5$ GeV [1], the QCDF approach [21] and the PQCD approach [22], but are larger than those given in the QCDSR [18] except that of the decay $J/\psi \to D_{(s)}K^{*+}$. While the branching ratios of the decays $J/\psi \to D_{(s)}P$ are in agreement with than the calculations given in the BSW model with the parameter $\omega = 0.4$ GeV [16], the PQCD approach [6] and the QCDF approach [21], while are smaller than those given in the NRQCD [5]. As to the $\psi(2S)$ decays, it is similar with the cases of the J/Ψ decays, that is the branching ratios of the decays $\psi(2S) \to D_{(s)}V$ are comparable with the current only available theoretical results in NRQCD [5], but those of the decays $\psi(2S) \to D_{(s)}P$ are much smaller. Certainly, the decays $J/\psi \to D_s^- \pi^+$, $J/\psi \to D^- \pi^+$, $J/\psi \to D_s^- \rho^+$ have been detected by the BESIII Collaboration but only with upper bounds [11,12] being available, which are much above all the theoretical predictions.

3. Whether the ground or radially excited charmonium state decays, there exists a clear hierarchical pattern among their branching ratios

$$\mathcal{B}r\left(\eta_c(nS) \to D_s^- \pi^+\right) \gg \mathcal{B}r\left(\eta_c(nS) \to D_s^- K^+\right)$$
$$\sim \mathcal{B}r\left(\eta_c(nS) \to D^- \pi^+\right) \gg \mathcal{B}r\left(\eta_c(nS) \to D^- K^+\right),$$

$$\mathcal{B}r\left(\psi(nS) \to D_s^- \pi^+\right) \gg \mathcal{B}r\left(\psi(nS) \to D_s^- K^+\right)$$
$$\sim \mathcal{B}r\left(\psi(nS) \to D^- \pi^+\right) \gg \mathcal{B}r\left(\psi(nS) \to D^- K^+\right),$$
$$\mathcal{B}r\left(\eta_c(nS) \to D_s^- \rho^+\right) \gg \mathcal{B}r\left(\eta_c(nS) \to D_s^- K^{*+}\right)$$
$$\sim \mathcal{B}r\left(\eta_c(nS) \to D^- \rho^+\right) \gg \mathcal{B}r\left(\eta_c(nS) \to D^- K^{*+}\right),$$
$$\mathcal{B}r\left(\psi(nS) \to D_s^- \rho^+\right) \gg \mathcal{B}r\left(\psi(nS) \to D_s^- K^{*+}\right)$$
$$\sim \mathcal{B}r\left(\psi(nS) \to D^- \rho^+\right) \gg \mathcal{B}r\left(\psi(nS) \to D^- K^{*+}\right),$$
$$(53)$$

which are primarily due to the hierarchical structures of CKM factors $V_{cs}V_{ud}(0.949) \gg V_{cs}V_{us}(0.219) \sim V_{cd}V_{ud}(0.215) \gg V_{cd}V_{us}(0.049)$.

4. Our primary focus lies on the nonleptonic decay channels that are most likely to be observed in future collider experiments. In Table 9, we list the ranges of the branching ratios for the Cabibbo-favored decays $\eta_c(1S, 2S) \to D_s^- \pi^+$, $\psi(1S, 2S) \to D_s^- \pi^+$, $\eta_c(1S, 2S) \to D_s^- \rho^+$, $\psi(1S, 2S) \to D_s^- \rho^+$ and the Cabibbo-suppressed decays $\eta_c(1S, 2S) \to D^- K^+$, $\psi(1S, 2S) \to D^- K^+$, $\eta_c(1S, 2S) \to D^- K^{*+}$, $\psi(1S, 2S) \to D^- K^{*+}$. It is obvious that the decays $\psi(1S, 2S) \to D_s^- \rho^+$ have the largest branching ratios and are most likely to be observed.

5. From our calculations, one can obtain the following relative ratios of the branching fractions where the uncertainties from the transition form factors are cancelled

$$R_{\eta_c}^{D_s} \equiv \frac{\mathcal{B}r(\eta_c \to D_s^- K^+)}{\mathcal{B}r(\eta_c \to D_s^- \pi^+)} = 0.063 \pm 0.012,$$

$$R_{\eta_c(2S)}^{D_s} \equiv \frac{\mathcal{B}r(\eta_c(2S) \to D_s^- K^+)}{\mathcal{B}r(\eta_c(2S) \to D_s^- \pi^+)} = 0.067 \pm 0.033,$$

$$R_{J/\psi}^{D_s} \equiv \frac{\mathcal{B}r(J/\psi \to D_s^- K^+)}{\mathcal{B}r(J/\psi \to D_s^- \pi^+)} = 0.055 \pm 0.020,$$

$$R_{\psi(2S)}^{D_s} \equiv \frac{\mathcal{B}r(\psi(2S) \to D_s^- K^+)}{\mathcal{B}r(\psi(2S) \to D_s^- \pi^+)} = 0.066 \pm 0.043.$$
$$(54)$$

$$R_{\eta_c}^{D} \equiv \frac{\mathcal{B}r(\eta_c \to D^- K^+)}{\mathcal{B}r(\eta_c \to D^- \pi^+)} = 0.070 \pm 0.010,$$

$$R_{\eta_c(2S)}^{D} \equiv \frac{\mathcal{B}r(\eta_c(2S) \to D^- K^+)}{\mathcal{B}r(\eta_c(2S) \to D^- \pi^+)} = 0.066 \pm 0.041,$$

$$R_{J/\psi}^{D} \equiv \frac{\mathcal{B}r(J/\psi \to D^- K^+)}{\mathcal{B}r(J/\psi \to D^- \pi^+)} = 0.061 \pm 0.011,$$

$$R^D_{\psi(2S)} \equiv \frac{\mathcal{B}r(\psi(2S) \to D^- K^+)}{\mathcal{B}r(\psi(2S) \to D^- \pi^+)} = 0.065 \pm 0.041,$$

$$(55)$$

which are consistent with the estimation $R = |V_{us}|^2 \frac{f_K^2}{f_\pi^2} \approx 0.074$ obtained from the factorization assumption. Furthermore, the ratios $R^{D_s}_{J/\psi}$ and $R^D_{J/\psi}$ agree well with the results 0.057 and 0.060 given in the QCDF [21]. Similarly, we can also define the ratios $R^\pi_{\eta_c(1S,2S)}$, $R^\pi_{\psi(1S,2S)}$ as follows

$$
\begin{aligned}
R^\pi_{\eta_c} &\equiv \frac{\mathcal{B}r(\eta_c \to D^- \pi^+)}{\mathcal{B}r(\eta_c \to D_s^- \pi^+)} \\
&= 0.050 \pm 0.006 \approx \left| \frac{V_{cd} F_0^{\eta_c D}(m_\pi^2)}{V_{cs} F_0^{\eta_c D_s}(m_\pi^2)} \right|^2 \\
&= 0.041,
\end{aligned}
$$

$$
\begin{aligned}
R^\pi_{\eta_c(2S)} &\equiv \frac{\mathcal{B}r(\eta_c(2S) \to D^- \pi^+)}{\mathcal{B}r(\eta_c(2S) \to D_s^- \pi^+)} \\
&= 0.040 \pm 0.019 \approx \left| \frac{V_{cd} F_0^{\eta_c(2S)D}(m_\pi^2)}{V_{cs} F_0^{\eta_c(2S)D_s}(m_\pi^2)} \right|^2 \\
&= 0.035,
\end{aligned}
$$

$$
\begin{aligned}
R^\pi_{J/\psi} &\equiv \frac{\mathcal{B}r(J/\psi \to D^- \pi^+)}{\mathcal{B}r(J/\psi \to D_s^- \pi^+)} \\
&= 0.052 \pm 0.015 \approx \left| \frac{V_{cd} A_0^{J/\psi D}(m_\pi^2)}{V_{cs} A_0^{J/\psi D_s}(m_\pi^2)} \right|^2 \\
&= 0.043,
\end{aligned}
$$

$$
\begin{aligned}
R^\pi_{\psi(2S)} &\equiv \frac{\mathcal{B}r(\psi(2S) \to D^- \pi^+)}{\mathcal{B}r(\psi(2S) \to D_s^- \pi^+)} \\
&= 0.061 \pm 0.040 \approx \left| \frac{V_{cd} A_0^{\psi(2S)D}(m_\pi^2)}{V_{cs} A_0^{\psi(2S)D_s}(m_\pi^2)} \right|^2 \\
&= 0.055.
\end{aligned}
$$

$$(56)$$

4 Summary

The charmonium weak decays provide a unique perspective on the underlying structures and dynamical mechanisms of hadrons and currents. With the anticipation of abundant data samples on charmonium at high-luminosity heavy-flavor experiments, we calculated some semileptonic and nonleptonic weak decays of charmonia $\eta_c(1S, 2S)$ and $\psi(1S, 2S)$ using the covariant light-front quark model. Here the nonperturbative weak transition form factors play a crucial role in evaluating the weak meson decay amplitudes. We extended analytically the expressions of the form factors of the transitions $\eta_c(1S, 2S) \to D_{(s)}$ and $\psi(1S, 2S) \to D_{(s)}$ in the space-like region to the time-like region using the double-pole model. The following are some points

1. In our considered decays, the channels $J/\psi \to D_s^- \ell^+ \nu_\ell$ and $J/\psi \to D_s^- \rho^+$ have the largest branching ratios, which are very close to or even upto 10^{-9}. These values are still much below the present experimental upper bounds.

2. The branching ratios for the semileptonic decays $J/\Psi \to D_{(s)}^- \ell^+ \nu_\ell$ are well consistent the results obtained from the BSW model, but some three or more times as large as those given by the BS approach, the CCQM and the QCDSR. The semileptonic decays of the radially excited charmonia $\psi(2S)$ and $\eta_c(2S)$ have not been studied by any other theory. We find that $Br(J/\Psi \to D_{(s)}^- \ell^+ \nu_\ell)$ are about three orders of magnitude larger than $Br(\eta_c \to D_{(s)}^- \ell^+ \nu_\ell)$, and $Br(\psi(2S) \to D_{(s)}^- \ell^+ \nu_\ell)$ are about two orders of magnitude larger than $Br(\eta_c(2S) \to D_{(s)}^- \ell^+ \nu_\ell)$.

3. Whether the semileptonic or the nonleptonic charmonium weak decays, the branching ratios for the ground state η_c decays are smaller than those of the radially excited state $\eta_c(2S)$ ones. It is contrary to the cases of $\psi(1S, 2S)$ decays, where the branching ratios of the ground sate J/Ψ decays are larger than those of the radially excited state $\psi(2S)$ ones. It is because of the larger (smaller) decay width of η_c (J/Ψ) compared with that of its radially excited state.

4. The ratios of the forward–backward asymmetries A^μ_{FB}/A^e_{FB} between the semileptonic decays $\eta_c(1S, 2S) \to D_{(s)}^- \mu^+ \nu_\mu$ and $\eta_c(1S, 2S) \to D_{(s)}^- e^+ \nu_e$ are in the order of 10^4, and the forward–backward asymmetries for the decays $\psi(1S, 2S) \to D_{(s)}^- \mu^+ \nu_\mu$ and $\psi(1S, 2S) \to D_{(s)}^- e^+ \nu_e$ become minus in sign and lies in the range of $(-0.3 \sim -0.2)$.

5. The longitudinal polarization fractions f_L are close to each other between the decays $\psi(1S, 2S) \to D_{(s)}^- e^+ \nu_e$ and $\psi(1S, 2S) \to D_{(s)}^- \mu^+ \nu_\mu$. Furthermore, the longitudinal and transverse polarization fractions for each decay are comparable.

6. Whether the ground or radially excited charmonium decays, the final states $D_s^- \pi^+ (D_s^- \rho^+)$ always own the largest yield and $D^- K^+ (D^- K^{*+})$ always have the smallest production, which are connected with the hierarchical structures of CKM factors, $V_{cs} V_{ud}(0.949) \gg V_{cd} V_{us}(0.049)$.

Data Availability Statement This manuscript has no associated data or the data will not be deposited. [Authors' comment: This work is a theoretical study. No relevant data to deposit].

Appendix A: Some specific rules under the p^- intergration

When preforming the integration, we need to include the zero-mode contribution. It amounts to performing the integration in a proper way in the CLFQM. Specificlly we use the following rules given in Refs. [24,30]

$$\hat{p}'_{1\mu} \doteq P_\mu A_1^{(1)} + q_\mu A_2^{(1)}, \tag{A1}$$

$$\hat{p}'_{1\mu}\hat{p}'_{1\nu} \doteq g_{\mu\nu} A_1^{(2)} + P_\mu P_\nu A_2^{(2)}$$
$$+ \left(P_\mu q_\nu + q_\mu P_\nu\right) A_3^{(2)} + q_\mu q_\nu A_4^{(2)}, \tag{A2}$$

$$Z_2 = \hat{N}'_1 + m_1'^2 - m_2^2 + (1 - 2x_1) M'^2$$
$$+ \left(q^2 + q\cdot P\right)\frac{p'_\perp \cdot q_\perp}{q^2}, \tag{A3}$$

$$\hat{p}'_{1\mu}\hat{N}_2 \rightarrow q_\mu \left[A_2^{(1)} Z_2 + \frac{q\cdot P}{q^2} A_1^{(2)}\right], \tag{A4}$$

$$\hat{p}'_{1\mu}\hat{p}'_{1\nu}\hat{N}_2 \rightarrow g_{\mu\nu} A_1^{(2)} Z_2$$
$$+ q_\mu q_\nu \left[A_4^{(2)} Z_2 + 2\frac{q\cdot P}{q^2} A_2^{(1)} A_1^{(2)}\right], \tag{A5}$$

$$A_1^{(1)} = \frac{x_1}{2}, \quad A_2^{(1)} = A_1^{(1)} - \frac{p'_\perp \cdot q_\perp}{q^2},$$

$$A_3^{(2)} = A_1^{(1)} A_2^{(1)},$$
$$A_4^{(2)} = \left(A_2^{(1)}\right)^2 - \frac{1}{q^2} A_1^{(2)}, \tag{A6}$$

$$A_1^{(2)} = -p'^2_\perp - \frac{\left(p'_\perp \cdot q_\perp\right)^2}{q^2},$$

$$A_2^{(2)} = \left(A_1^{(1)}\right)^2. \tag{A7}$$

Appendix B: Expressions of $\eta_c(\psi) \rightarrow D_{(s)}$ form factors

$$S_\mu^{\eta_c D_{(s)}} = \mathrm{Tr}\left[\gamma_5 \left(\slashed{p}''_1 + m''_1\right)\gamma_\mu \left(\slashed{p}'_1 + m'_1\right)\gamma_5 \left(-\slashed{p}_2 + m_2\right)\right]$$
$$= 2p'_{1\mu}\left[M'^2 + M''^2 - q^2 - 2N_2 - \left(m'_1 - m_2\right)^2\right.$$
$$\left. - \left(m''_1 - m_2\right)^2 + \left(m'_1 - m''_1\right)^2\right]$$
$$+ q_\mu\left[q^2 - 2M'^2 + N'_1 - N''_1\right.$$

$$\left. + 2N_2 + 2\left(m'_1 - m_2\right)^2 - \left(m'_1 - m''_1\right)^2\right]$$
$$+ P_\mu\left[q^2 - N'_1 - N''_1 - \left(m'_1 - m''_1\right)^2\right], \tag{B1}$$

$$S_{\mu\nu}^{\psi D_{(s)}} = \left(S_V^{\psi D_{(s)}} - S_A^{\psi D_{(s)}}\right)_{\mu\nu}$$
$$= \mathrm{Tr}\left[\left(\gamma_\nu - \frac{1}{W''_V}\left(p''_1 - p_2\right)_\nu\right)\left(\slashed{p}''_1 + m''_1\right)\right.$$
$$\left.\left(\gamma_\mu - \gamma_\mu\gamma_5\right)\left(\slashed{p}'_1 + m'_1\right)\gamma_5\left(-\slashed{p}_2 + m_2\right)\right]$$
$$= -2i\epsilon_{\mu\nu\alpha\beta}\left\{p_1'^\alpha P^\beta\left(m''_1 - m'_1\right)\right.$$
$$\left. + p_1'^\alpha q^\beta\left(m''_1 + m'_1 - 2m_2\right) + q^\alpha P^\beta m'_1\right\}$$
$$+ \frac{1}{W''_V}\left(4p'_{1\nu} - 3q_\nu - P_\nu\right)i\epsilon_{\mu\alpha\beta\rho}p_1'^\alpha q^\beta P^\rho$$
$$+ 2g_{\mu\nu}\left\{m_2\left(q^2 - N'_1 - N''_1 - m_1'^2 - m_1''^2\right)\right.$$
$$- m'_1\left(M''^2 - N''_1 - N_2 - m_1''^2 - m_2^2\right)$$
$$\left. - m''_1\left(M'^2 - N'_1 - N_2 - m_1'^2 - m_2^2\right) - 2m'_1 m''_1 m_2\right\}$$
$$+ 8p'_{1\mu}p'_{1\nu}\left(m_2 - m'_1\right) - 2\left(P_\mu q_\nu + q_\mu P_\nu + 2q_\mu q_\nu\right)m'_1$$
$$+ 2p'_{1\mu}P_\nu\left(m'_1 - m''_1\right)$$
$$+ 2p'_{1\mu}q_\nu\left(3m'_1 - m''_1 - 2m_2\right) + 2P_\mu p'_{1\nu}\left(m'_1 + m''_1\right)$$
$$+ 2q_\mu p'_{1\nu}\left(3m'_1 + m''_1 - 2m_2\right)$$
$$+ \frac{1}{2W''_V}\left(4p'_{1\nu} - 3q_\nu - P_\nu\right)\left\{2p'_{1\mu}\left[M'^2 + M''^2 - q^2\right.\right.$$
$$\left. - 2N_2 + 2\left(m'_1 - m_2\right)\left(m''_1 + m_2\right)\right]$$
$$+ q_\mu\left[q^2 - 2M'^2 + N'_1 - N''_1 + 2N_2 - \left(m'_1 + m''_1\right)^2\right.$$
$$\left. + 2\left(m'_1 - m_2\right)^2\right]$$
$$\left.\left. + P_\mu\left[q^2 - N'_1 - N''_1 - \left(m'_1 + m''_1\right)^2\right]\right\}\right\}. \tag{B2}$$

The following are the analytical expressions of the form factors of transitions $\eta_c(1 S, 2 S) \rightarrow D_{(s)}$, $\psi(1 S, 2 S) \rightarrow (1 S, 2 S) \rightarrow D_{(s)}$ in the covariant light-front quark model

$$F_1^{\eta_c D_{(s)}}\left(q^2\right) = \frac{N_c}{16\pi^3}\int dx_2 d^2$$
$$p'_\perp \frac{h'_{\eta_c}h''_{D_{(s)}}}{x_2\hat{N}'_1\hat{N}''_1}\left[x_1\left(M_0'^2 + M_0''^2\right) + x_2 q^2 - x_2\left(m'_1 - m''_1\right)^2\right.$$
$$\left. - x_1\left(m'_1 - m_2\right)^2 - x_1\left(m''_1 - m_2\right)^2\right] \tag{B3}$$

$$F_0^{\eta_c D_{(s)}}\left(q^2\right) = F_1^{\eta_c D_{(s)}}(q^2) + \frac{q^2}{(q\cdot P)}\frac{N_c}{16\pi^3}$$
$$\times \int dx_2 d^2 p'_\perp \frac{2h'_{\eta_c}h''_{D_{(s)}}}{x_2\hat{N}'_1\hat{N}''_1}\left\{-x_1 x_2 M'^2 - p'^2_\perp - m'_1 m_2\right.$$
$$+ \left(m''_1 - m_2\right)\left(x_2 m'_1 + x_1 m_2\right)$$
$$+ 2\frac{q\cdot P}{q^2}\left(p'^2_\perp + 2\frac{\left(p'_\perp \cdot q_\perp\right)^2}{q^2}\right) + 2\frac{\left(p'_\perp \cdot q_\perp\right)^2}{q^2}$$
$$- \frac{p'_\perp \cdot q_\perp}{q^2}\left[M''^2 - x_2\left(q^2 + q\cdot P\right)\right.$$
$$\left. - \left(x_2 - x_1\right)M'^2 + 2x_1 M_0'^2\right.$$
$$\left. - 2\left(m'_1 - m_2\right)\left(m'_1 + m''_1\right)\right]\right\}, \tag{B4}$$

$$V^{\psi D_{(s)}}(q^2) = \frac{N_c(M' + M'')}{16\pi^3} \int dx_2 d^2$$

$$p'_\perp \frac{2h'_\psi h''_{D_{(s)}}}{x_2 \hat{N}'_1 \hat{N}''_1} \left\{ x_2 m'_1 + x_1 m_2 + (m'_1 - m''_1) \frac{p'_\perp \cdot q_\perp}{q^2} \right.$$

$$\left. + \frac{2}{w''_V} \left[p'^2_\perp + \frac{(p'_\perp \cdot q_\perp)^2}{q^2} \right] \right\}, \tag{B5}$$

$$A_0^{\psi D_{(s)}}(q^2) = \frac{M' + M''}{2M''} A_1^{\psi D_{(s)}}(q^2) - \frac{M' - M''}{2M''} A_2^{\psi D_{(s)}}(q^2)$$

$$- \frac{q^2}{2M''} \frac{N_c}{16\pi^3}$$

$$\times \int dx_2 d^2 p'_\perp \frac{h'_\psi h''_{D_{(s)}}}{x_2 \hat{N}'_1 \hat{N}''_1} \{2(2x_1 - 3)$$

$$(x_2 m'_1 + x_1 m_2) - 8(m'_1 - m_2)$$

$$\times \left[\frac{p'^2_\perp}{q^2} + 2 \frac{(p'_\perp \cdot q_\perp)^2}{q^4} \right] - \left[(14 - 12x_1) m'_1 \right.$$

$$\left. - 2m''_1 - (8 - 12x_1) m_2 \right] \frac{p'_\perp \cdot q_\perp}{q^2} + \frac{4}{w''_V}$$

$$\times \left(\left[M'^2 + M''^2 - q^2 + 2(m'_1 - m_2)(m''_1 + m_2) \right] \right.$$

$$\times \left(A_3^{(2)} + A_4^{(2)} - A_2^{(1)} \right) + Z_2 \left(3A_2^{(1)} - 2A_4^{(2)} - 1 \right)$$

$$+ \frac{1}{2} \left[x_1 (q^2 + q \cdot P) - 2M'^2 - 2p'_\perp \cdot q_\perp \right.$$

$$\left. - 2m'_1 (m''_1 + m_2) - 2m_2 (m'_1 - m_2) \right]$$

$$\left(A_1^{(1)} + A_2^{(1)} - 1 \right) q \cdot P \left[\frac{p'^2_\perp}{q^2} + \frac{(p'_\perp \cdot q_\perp)^2}{q^4} \right]$$

$$\left. \times \left(4A_2^{(1)} - 3 \right) \right) \Big\}, \tag{B6}$$

$$A_1^{\psi D_{(s)}}(q^2) = -\frac{1}{M' + M''} \frac{N_c}{16\pi^3} \int dx_2 d^2$$

$$p'_\perp \frac{h'_\psi h''_{D_{(s)}}}{x_2 \hat{N}'_1 \hat{N}''_1} \left\{ 2x_1 (m_2 - m'_1)(M'^2_0 + M''^2_0) - 4x_1 m''_1 M'^2_0 \right.$$

$$+ 2x_2 m'_1 q \cdot P + 2m_2 q^2 - 2x_1 m_2 (M'^2 + M''^2)$$

$$+ 2(m'_1 - m_2)(m'_1 + m''_1)^2 + 8(m'_1 - m_2)$$

$$\times \left[p'^2_\perp + \frac{(p'_\perp \cdot q_\perp)^2}{q^2} \right] + 2(m'_1 + m''_1)(q^2 + q \cdot P) \frac{p'_\perp \cdot q_\perp}{q^2}$$

$$- 4 \frac{q^2 p'^2_\perp + (p'_\perp \cdot q_\perp)^2}{q^2 w''_V}$$

$$\times \left[2x_1 (M'^2 + M'^2_0) - q^2 - q \cdot P - 2(q^2 + q \cdot P) \frac{p'_\perp \cdot q_\perp}{q^2} \right.$$

$$\left. - 2(m'_1 - m''_1)(m'_1 - m_2) \right] \Big\}, \tag{B7}$$

$$A_2^{\psi D_{(s)}}(q^2) = \frac{N_c(M' + M'')}{16\pi^3} \int dx_2 d^2 p'_\perp \frac{2h'_\psi h''_{D_{(s)}}}{x_2 \hat{N}'_1 \hat{N}''_1}$$

$$\times \left\{ (x_1 - x_2)(x_2 m'_1 + x_1 m_2) - \frac{p'_\perp \cdot q_\perp}{q^2} \left[2x_1 m_2 + m''_1 \right. \right.$$

$$\left. + (x_2 - x_1) m'_1 \right] - 2 \frac{x_2 q^2 + p'_\perp \cdot q_\perp}{x_2 q^2 w''_V}$$

$$\left. \times \left[p'_\perp \cdot p''_\perp + (x_1 m_2 + x_2 m'_1)(x_1 m_2 - x_2 m''_1) \right] \right\}. \tag{B8}$$

References

1. K.K. Sharma, R.C. Verma, Int. J. Mod. Phys. A **14**, 937 (1999). arXiv:hep-ph/9801202
2. R.C. Verma, A.N. Kamal, A. Czarnecki, Phys. Lett. B **252**, 690 (1990)
3. Y.M. Wang, H. Zou, Z.T. Wei, X.Q. Li, C.D. Lu, Eur. Phys. J. C **54**, 107 (2008). arXiv:0707.1138 [hep-ph]
4. Y.M. Wang, H. Zou, Z.T. Wei, X.Q. Li, C.D. Lu, Eur. Phys. J. C **55**, 607 (2008). arXiv:0802.2762 [hep-ph]
5. J. Sun, Y. Yang, J. Huang, L. Chen, Q. Chang, Adv. High Energy Phys. **2016**, 5071671 (2016). arXiv:1511.03420 [hep-ph]
6. J. Sun, Y. Yang, J. Gao, Q. Chang, J. Huang, G. Lu, Phys. Rev. D **94**, 034029 (2016). arXiv:1709.05080 [hep-ph]
7. S. Okubo, Phys. Lett. **5**, 165 (1963)
8. G. Zweig, CERN-TH-401, 412 (1964)
9. J. Iizuka, Prog. Theor. Phys. Suppl. **37**, 21 (1966)
10. M.A. Sanchis-Lozano, Z. Phys. C **62**, 271 (1994)
11. M. Ablikim et al. [BES], Phys. Lett. B **663**, 297 (2008). arXiv:0707.3005 [hep-ex]
12. M. Ablikim et al. [BESIII], Phys. Rev. D **89**, 071101 (2014). arXiv:1402.4025 [hep-ex]
13. M. Ablikim et al. [BESIII], Phys. Rev. D **90**, 112014 (2014). arXiv:1410.8426 [hep-ex]
14. M. Ablikim et al. [BESIII], JHEP **06**, 157 (2021). arXiv:2104.06628 [hep-ex]
15. M. Ablikim et al. [BESIII]. arXiv:2307.02165 [hep-ex]
16. R. Dhir, R. Verma, A. Sharma, Adv. High Energy Phys **2013**, 706543 (2013). arXiv:0903.1201 [hep-ph]
17. Y.L. Shen, Y.M. Wang, Phys. Rev. D **78**, 074012 (2008)
18. Y.M. Wang, H. Zou, Z.T. Wei, X.Q. Li, C.D. Lu, Eur. Phys. J. C **55**, 607 (2008). arXiv:0802.2762 [hep-ph]
19. T. Wang, Y. Jiang, H. Yuan, K. Chai, G.L. Wang, J. Phys. G **44**, 045004 (2017). arXiv:1604.03298 [hep-ph]
20. Y.M. Wang, H. Zou, Z.T. Wei, X.Q. Li, C.D. Lu, Eur. Phys. J. C **54**, 107 (2008). arXiv:0707.1138 [hep-ph]
21. J. Sun, L. Chen, Q. Chang, J. Huang, Y. Yang, Int. J. Mod. Phys. A **30**, 1550094 (2015). arXiv:1603.00130 [hep-ph]
22. Y. Yang, J. Sun, J. Gao, Q. Chang, J. Huang, G. Lu, Int. J. Mod. Phys. A **31**, 1650161 (2016). arXiv:1709.10220 [hep-ph]
23. M.A. Ivanov, C.T. Tran, Phys. Rev. D **92**, 074030 (2015). arXiv:1701.07377 [hep-ph]
24. H.Y. Cheng, C.K. Chua, C.W. Hwang, Phys. Rev. D **69**, 074025 (2004). arXiv:hep-ph/0310359
25. H.Y. Cheng, C.K. Chua, Phys. Rev. D **69**, 094007 (2004). arXiv:hep-ph/0401141. [erratum: Phys. Rev. D 81, 059901 (2010)]
26. C.W. Hwang, Z.T. Wei, J. Phys. G **34**, 687 (2007). arXiv:hep-ph/0609036
27. C.D. Lu, W. Wang, Z.T. Wei, Phys. Rev. D **76**, 014013 (2007). arXiv:hep-ph/0701265
28. W. Wang, Y.L. Shen, C.D. Lu, Eur. Phys. J. C **51**, 841 (2007). arXiv:0704.2493 [hep-ph]
29. Z.Q. Zhang, Z.J. Sun, Y.C. Zhao, Y.Y. Yang, Z.Y. Zhang, Eur. Phys. J. C **83**, 477 (2023). arXiv:2301.11107 [hep-ph]
30. W. Jaus, Phys. Rev. D **60**, 054026 (1999)
31. Y. Sakaki, M. Tanaka, A. Tayduganov, R. Watanabe, Phys. Rev. D **88**, 094012 (2013). arXiv:1309.0301 [hep-ph]
32. G. Buchalla, A. Buras, M. Lautenbacher, Rev. Mod. Phys. **68**, 1125 (1996). arXiv:hep-ph/9512380
33. R.L. Workman et al. [Particle Data Group], Review of particle physics. PTEP **2022**, 083C01 (2022)
34. D. Bečirević, G. Duplančić, B. Klajn, B. Melić, Nucl. Phys. B **883**, 306 (2014). arXiv:1312.2858 [hep-ph]
35. T.W. Chiu, T.H. Hsieh, J.Y. Lee, P.H. Liu, H.J. Chang, Phys. Lett. B **624**, 31 (2005). arXiv:hep-ph/0506266

36. M. Wingate, C.T.H. Davies, A. Gray, G.P. Lepage, J. Shigemitsu, Phys. Rev. Lett. **92**, 162001 (2004). arXiv:hep-ph/0311130
37. D. Bečirević, G. Duplančić, B. Klajn, B. Melić, F. Sanfilippo, Nucl. Phys. B **883**, 306 (2014)
38. D.M. Asner et al. [CLEO Collaboration], Phys. Rev. Lett. **92**, 142001 (2004). arXiv:hep-ex/0312058
39. Z.Z. Song, C. Meng, K.T. Chao, Eur. Phys. J. C **36**, 365 (2004). arXiv:hep-ph/0209257
40. Z.J. Sun, S.Y. Wang, Z.Q. Zhang, Y.Y. Yang, Z.Y. Zhang, Eur. Phys. J. C **83**, 945 (2023). arXiv:2308.03114 [hep-ph]